

---

---

**Information technology — Biometric  
sample quality —**

**Part 4:  
Finger image data**

*Technologies de l'information — Qualité d'échantillon biométrique —  
Partie 4: Données d'image de doigt*

STANDARDSISO.COM : Click to view the full PDF of ISO/IEC 29794-4:2017



STANDARDSISO.COM : Click to view the full PDF of ISO/IEC 29794-4:2017



**COPYRIGHT PROTECTED DOCUMENT**

© ISO/IEC 2017, Published in Switzerland

All rights reserved. Unless otherwise specified, no part of this publication may be reproduced or utilized otherwise in any form or by any means, electronic or mechanical, including photocopying, or posting on the internet or an intranet, without prior written permission. Permission can be requested from either ISO at the address below or ISO's member body in the country of the requester.

ISO copyright office  
Ch. de Blandonnet 8 • CP 401  
CH-1214 Vernier, Geneva, Switzerland  
Tel. +41 22 749 01 11  
Fax +41 22 749 09 47  
copyright@iso.org  
www.iso.org

# Contents

	Page
<b>Foreword</b> .....	<b>iv</b>
<b>Introduction</b> .....	<b>v</b>
<b>1 Scope</b> .....	<b>1</b>
<b>2 Normative references</b> .....	<b>1</b>
<b>3 Terms, definitions, symbols and abbreviated terms</b> .....	<b>1</b>
<b>4 Conformance</b> .....	<b>2</b>
<b>5 Finger image quality metrics</b> .....	<b>2</b>
5.1 Overview.....	2
5.1.1 General.....	2
5.1.2 Constituent of local quality metrics.....	3
5.1.3 Constituent of global quality metrics.....	3
5.1.4 Image preprocessing.....	3
5.1.5 Image examples.....	5
5.2 Normative contributive quality metrics.....	5
5.2.1 General.....	5
5.2.2 Orientation certainty level.....	5
5.2.3 Local clarity score.....	7
5.2.4 Frequency domain analysis (FDA) score.....	11
5.2.5 Ridge valley uniformity.....	13
5.2.6 Orientation flow.....	14
5.2.7 MU.....	15
5.2.8 MMB.....	15
5.2.9 Minutiae count in finger image.....	16
5.2.10 Minutiae count in center of mass region.....	16
5.2.11 Minutiae quality based on local image mean.....	16
5.2.12 Minutiae quality based on local orientation certainty level.....	17
5.2.13 Region of interest image mean.....	17
5.2.14 Region of interest orientation map coherence sum.....	19
5.2.15 Region of interest relative orientation map coherence sum.....	20
5.2.16 Quality feature vector composition.....	20
5.3 Non-normative quality metrics.....	23
5.3.1 General.....	23
5.3.2 Radial power spectrum.....	23
5.3.3 Gabor quality score.....	25
5.4 Unified quality score.....	27
5.4.1 Methodology for combining quality metrics.....	27
5.4.2 Training method.....	27
<b>6 Finger image quality data record</b> .....	<b>28</b>
6.1 Binary encoding.....	28
6.2 XML encoding.....	29
6.3 Quality algorithm identifiers.....	30
<b>Annex A (normative) Conformance test assertions</b> .....	<b>32</b>
<b>Annex B (informative) Factors influencing fingerprint image character</b> .....	<b>44</b>
<b>Annex C (informative) Area consideration</b> .....	<b>46</b>
<b>Bibliography</b> .....	<b>47</b>

## Foreword

ISO (the International Organization for Standardization) and IEC (the International Electrotechnical Commission) form the specialized system for worldwide standardization. National bodies that are members of ISO or IEC participate in the development of International Standards through technical committees established by the respective organization to deal with particular fields of technical activity. ISO and IEC technical committees collaborate in fields of mutual interest. Other international organizations, governmental and non-governmental, in liaison with ISO and IEC, also take part in the work. In the field of information technology, ISO and IEC have established a joint technical committee, ISO/IEC JTC 1.

The procedures used to develop this document and those intended for its further maintenance are described in the ISO/IEC Directives, Part 1. In particular the different approval criteria needed for the different types of ISO documents should be noted. This document was drafted in accordance with the editorial rules of the ISO/IEC Directives, Part 2 (see [www.iso.org/directives](http://www.iso.org/directives)).

Attention is drawn to the possibility that some of the elements of this document may be the subject of patent rights. ISO shall not be held responsible for identifying any or all such patent rights. Details of any patent rights identified during the development of the document will be in the Introduction and/or on the ISO list of patent declarations received (see [www.iso.org/patents](http://www.iso.org/patents)).

Any trade name used in this document is information given for the convenience of users and does not constitute an endorsement.

For an explanation on the voluntary nature of standards, the meaning of ISO specific terms and expressions related to conformity assessment, as well as information about ISO's adherence to the World Trade Organization (WTO) principles in the Technical Barriers to Trade (TBT) see the following URL: [www.iso.org/iso/foreword.html](http://www.iso.org/iso/foreword.html).

This document was prepared by Joint Technical Committee ISO/IEC JTC 1, *Information technology*, Subcommittee SC 37, *Biometrics*.

This first edition cancels and replaces ISO/IEC/TR 29794-4:2010, which has been technically revised to become an International Standard.

A list of all parts in the ISO 29794 series can be found on the ISO website.

## Introduction

This document specifies finger image quality metrics. A reference implementation of the normative metrics is available at <https://github.com/usnistgov/NFIQ2>.

The quality of finger image data is defined to be the degree to which the finger image data fulfils specified requirements for the targeted application. Thus, the quality information is useful in many applications. ISO/IEC 19784-1 allocates a quality field and specifies the allowable range for the scores, with a recommendation that the score be divided into four categories with a qualitative interpretation for each category. Image quality fields are also provided in the fingerprint data interchange formats standardized in ISO/IEC 19794-2, ISO/IEC 19794-3, ISO/IEC 19794-4, and ISO/IEC 19794-8. This document defines a standard way to calculate the finger image quality score that facilitates the interpretation and interchange of the finger image quality scores.

STANDARDSISO.COM : Click to view the full PDF of ISO/IEC 29794-4:2017

# Information technology — Biometric sample quality —

## Part 4: Finger image data

### 1 Scope

This document establishes

- terms and definitions for quantifying finger image quality,
- methods used to quantify the quality of finger images, and
- standardized encoding of finger image quality,

for finger images at 196,85 px/cm spatial sampling rate scanned or captured using optical sensors with capture dimension (width, height) of at least 1,27 cm × 1,651 cm.

### 2 Normative references

The following documents are referred to in the text in such a way that some or all of their content constitutes requirements of this document. For dated references, only the edition cited applies. For undated references, the latest edition of the referenced document (including any amendments) applies.

ISO/IEC 2382-37, *Information technology — Vocabulary — Part 37: Biometrics*

ISO/IEC 19794-1:2011, *Information technology — Biometric data interchange formats — Part 1: Framework*

ISO/IEC 29794-1, *Information technology — Biometric sample quality — Part 1: Framework*

### 3 Terms, definitions, symbols and abbreviated terms

#### 3.1 Terms and definitions

For the purposes of this document, the terms and definitions given in ISO/IEC 2382-37, ISO/IEC 29794-1 and the following apply.

ISO and IEC maintain terminological databases for use in standardization at the following addresses:

- IEC Electropedia: available at <http://www.electropedia.org/>
- ISO Online browsing platform: available at <http://www.iso.org/obp>

##### 3.1.1

##### **foreground region**

set of all pixels of a finger image that form valid finger image patterns

Note 1 to entry: The most evident structural characteristic of a valid finger image is a pattern of interleaved ridges and valleys.

### 3.1.2

#### **local region**

block of  $m \times n$  pixels of the foreground of a finger image, where  $m$  and  $n$  are smaller than or equal to the width and the height of the finger image

### 3.1.3

#### **finger image quality assessment algorithm**

algorithm that reports a quality score for a given finger image

### 3.1.4

#### **metric**

quantification of a covariate using a prescribed method

### 3.1.5

#### **covariate**

variable or parameter that either directly, or when interacting with other covariates, affects fingerprint recognition accuracy

## 3.2 Symbols and abbreviated terms

DFT Discrete Fourier Transform

$I$  matrix of grey-level intensity values corresponding to the pixels of an image

$S$  ridge valley signature of a local region  $V$

$V$  matrix of grey-level intensity values corresponding to the pixels of a local region

## 4 Conformance

A finger image quality assessment algorithm conforms to this document if it conforms to the normative requirements of [Clause 5](#).

A finger image quality record shall conform to this document if its structure and data values conform to the formatting requirements of [Clause 6](#) (finger image quality data record) and its quality values are computed using the methods specified in [5.2](#), [5.3](#) and [5.4](#).

Conformance to normative requirements of [Clause 6](#) fulfils Level 1 and Level 2 conformance as specified in ISO/IEC 19794-1:2011, Annex A. Conformance to normative requirements of [5.2](#) and [5.4](#) is Level 3 conformance as specified in ISO/IEC 19794-1:2011, Annex A.

## 5 Finger image quality metrics

### 5.1 Overview

#### 5.1.1 General

[Clause 5](#) establishes metrics for predicting the utility of a finger image ([5.2](#) and [5.3](#)). Image quality metrics from a single image are useful to ensure the acquired image is suitable for recognition.

A complete finger image quality analysis shall examine both the local and global structures of the finger image. Fingerprint local structure constitutes the main texture-like pattern of ridges and valleys within a local region while valid global structure puts the ridges and valleys into a smooth flow for the entire fingerprint. The quality of a finger image is determined by both its local and global structures. [Clause 5](#) describes the features and characteristics of finger images at both local and global structures that are to be used for quantifying finger image quality.

For applying the algorithms as described in 5.2 and 5.3, the finger image shall have a spatial sampling rate of 196,85 pixels per centimetre (500 pixels per inch).

### 5.1.2 Constituent of local quality metrics

A finger image is partitioned into local regions such that each local region contains sufficient ridge-valley information, preferably having at least 2 clear ridges, while not overly constraining the high curvature ridges. For images with a spatial sampling rate of 196,85 pixel per centimetre (500 pixel per inch), the ridge separation usually varies between 8 pixels to 12 pixels<sup>[1]</sup>. A ridge separation comprises a ridge and a valley. In order to cover two clear ridges, the local region size has to be greater than 24 pixels in both width and height. The size for each local region shall be  $32 \times 32$  pixels, which is sufficient to cover 2 clear ridges. Instead of Cartesian coordinate, curvilinear coordinate along the ridge can also be used.

### 5.1.3 Constituent of global quality metrics

A global quality metric should be computed over the whole image and assess the utility of fingerprint characteristics in the image.

### 5.1.4 Image preprocessing

#### 5.1.4.1 Description

A segmentation process follows where each local region is labelled as background or foreground. There are several segmentation approaches, such as using the average magnitude of the pixel-intensity gradient in each local region<sup>[1]</sup>.

This document does not prescribe segmentation methods, but notes that performing segmentation influences the computed scores. Constant or near constant areas of the input image shall be removed according to 5.1.4.2 prior to computing quality using the metrics specified in 5.2 and 5.3.

#### 5.1.4.2 Removal of near constant white lines in image

Prior to computing features, fingerprint images are cropped to remove white pixels on the margins. Starting from the outer margins, rows and columns with average pixel intensity above 250 are removed.

Pixel intensities take values  $[0, 255]$  for an 8-bit gray scale image. As a first approximation of the region of interest, image columns and rows which are near constant white background are removed. Using the algorithm specified below, a fixed threshold is set for gray scale pixel intensity of  $T_\mu = 250$  to obtain the image without near constant areas.

The algorithm is specified as:

- a) For each row  $R_i$  in  $I$ , starting from the top
  - 1) Compute the row arithmetic mean  $\mu_{\text{row}}$
  - 2) On the first occurrence where  $\mu_{\text{row}} \leq T_\mu$  set  $idx_t = i$
  - 3) On the last occurrence where  $\mu_{\text{row}} \leq T_\mu$  set  $idx_b = i$
- b) For each column  $C_j$  in  $I$ , starting from the left
  - 1) Compute the column arithmetic mean  $\mu_{\text{col}}$
  - 2) On the first occurrence where  $\mu_{\text{col}} \leq T_\mu$  set  $idx_l = i$
  - 3) On the last occurrence where  $\mu_{\text{col}} \leq T_\mu$  set  $idx_r = i$
- c) Extract the region of interest as  $\hat{I} = I.\text{roi}(idx_l, idx_t, idx_r, idx_b)$

**5.1.4.3 Foreground segmentation based on local standard deviation**

For quality features which require a foreground mask to indicate regions containing the fingerprint an algorithm using local standard deviation is adopted.

The algorithm is specified as:

- a) Normalize  $I$  to zero mean and unit standard deviation to produce  $\hat{I}$
- b) For each local region  $V$  in  $\hat{I}$ 
  - 1) Compute the standard deviation of  $V$  as  $\sigma_V$
  - 2) Mark the corresponding local region in  $I_{\text{mask}}$  as foreground if  $\sigma_V > 0,1$

**5.1.4.4 Computing the dominant ridge flow orientation for a local region from pixel-intensity gradients**

The dominant ridge flow orientation is determined by computing the pixel-intensity gradient information and then determining the orientation of the principal variation axis.

The numerical gradient of the local region is determined using finite central difference for all interior pixels in x-direction and y-direction

$$f_x = \frac{I(x+1, y) - I(x-1, y)}{2} \tag{1}$$

$$f_y = \frac{I(x, y+1) - I(x, y-1)}{2} \tag{2}$$

With  $f_x$  and  $f_y$ , the dominant ridge flow orientation,  $angle(V)$ , is determined analytically using the sine and cosine doubled angle determined from the arithmetic means of the pixel-intensity gradient covariances.

$$a = \overline{f_x^2} \tag{3}$$

$$b = \overline{f_y^2} \tag{4}$$

$$c = \overline{f_x f_y} \tag{5}$$

$$C = \begin{bmatrix} a & c \\ c & b \end{bmatrix} \tag{6}$$

$$d = \sqrt{c^2 + (a-b)^2} + \epsilon \tag{7}$$

$$\sin \theta = \frac{c}{d} \tag{8}$$

$$\cos \theta = \frac{a-b}{d} \tag{9}$$

$$angle(V) = \frac{1}{2} \tan^{-1} \frac{\sin \theta}{\cos \theta} \tag{10}$$

### 5.1.5 Image examples

For algorithms operating in a block-wise manner the input image is subdivided into local regions according to the overlay grid shown in [Figure 1 b\)](#). The local region  $V(8,5)$  is used as example in local processing and is marked up using a bold line. [Figure 1 c\)](#) shows an enlarged view of  $V(8,5)$  and [Figure 1 d\)](#) shows  $V(8,5)$  rotated according to its dominant ridge orientation computed using [Formula \(10\)](#).

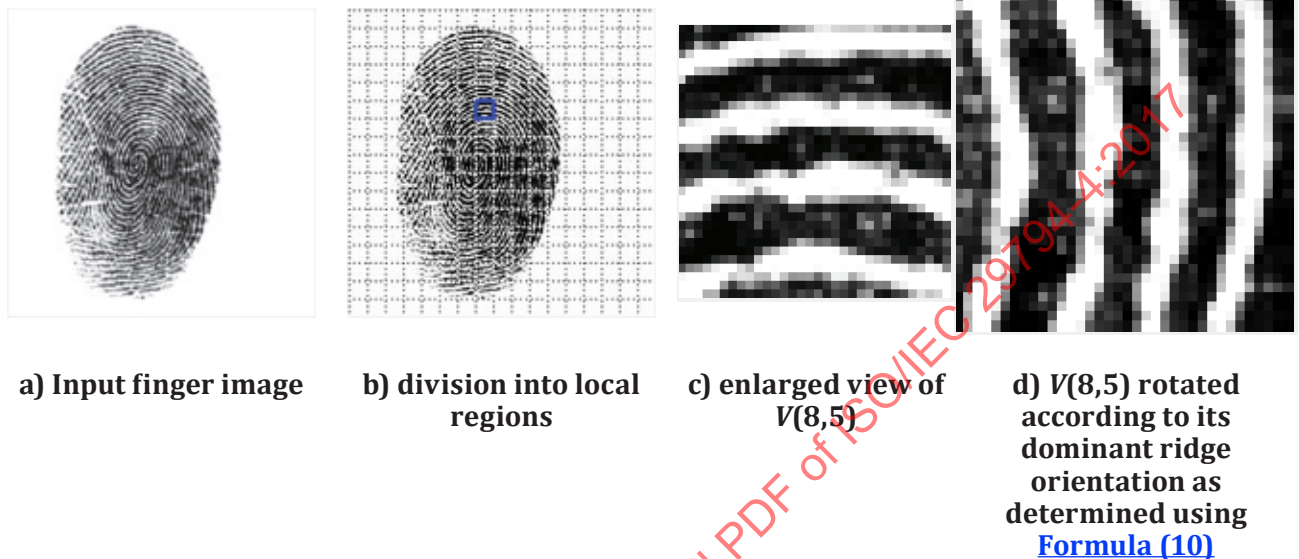


Figure 1 — Input image used — Examples of the processing of quality

## 5.2 Normative contributive quality metrics

### 5.2.1 General

[5.2](#) specifies normative contributive finger image quality assessment algorithms.

### 5.2.2 Orientation certainty level

#### 5.2.2.1 Description

The orientation certainty level (OCL)<sup>[3]</sup> of a local region is a measure of the consistency of the orientations of the ridges and valleys contained within this local region. The feature computes local quality and operates in a block-wise manner.

The finger image within a  $32 \times 32$  pixels local region [as shown in [Figure 1 c\)](#)] generally consists of dark ridge lines separated by white valley lines along the same orientation. The consistent ridge orientation and the appropriate ridge and valley structure are distinguishable local characteristics of the fingerprint local region.

The pixel-intensity gradient  $(dx, dy)$  at a pixel describes the direction of the maximum pixel-intensity change and its strength. By performing Principal Component Analysis on the pixel-intensity gradients in a local region, an orthogonal basis for the local region can be formed by finding its eigenvalues and eigenvectors. The resultant first principal component contains the largest variance contributed by the maximum total gradient change in the direction orthogonal to ridge orientation. The direction is given by the first eigenvector and the value of the variance corresponds to the first eigenvalue,  $\lambda_{\max}$ . On the other hand, the resultant second principal component has the minimum change of gradient in the direction of ridge flow which corresponds to the second eigenvalue,  $\lambda_{\min}$ . The ratio between the two eigenvalues thus gives an indication of how strong the energy is concentrated along the dominant

direction with two vectors pointing to the normal and tangential direction of the average ridge flow respectively.

**5.2.2.2 Computing the eigenvalues and local orientation certainty**

From the covariance matrix  $C$  [Formula (6)] the eigenvalues  $\lambda_{\min}$  and  $\lambda_{\max}$  are computed as

$$\lambda_{\min} = \frac{a+b-\sqrt{(a-b)^2+4c^2}}{2} \tag{11}$$

$$\lambda_{\max} = \frac{a+b+\sqrt{(a-b)^2+4c^2}}{2} \tag{12}$$

which yields a local orientation certainty level

$$Q_{\text{OCL}}^{\text{local}} = \begin{cases} 1 - \frac{\lambda_{\min}}{\lambda_{\max}}, & \text{if } \lambda_{\max} > 0 \\ 0, & \text{otherwise} \end{cases} \tag{13}$$

which is a ratio in the interval [0,1] where 1 is highest certainty level and 0 is lowest.

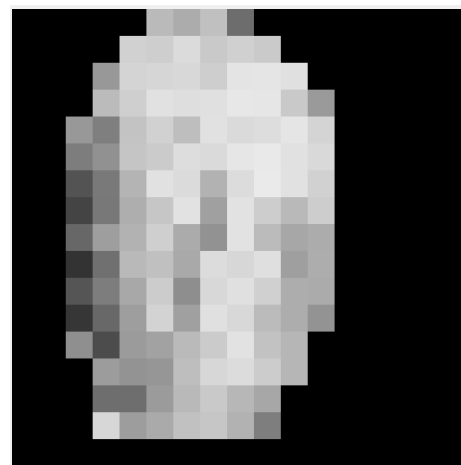
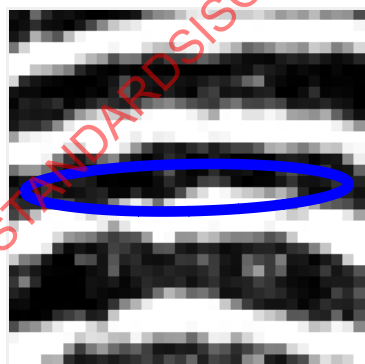
NOTE The orientation certainty level fails to predict match-ability when some marks or residual exist in the samples that have strong orientation strength, such as those exhibited by latent prints left by the previous user.

**5.2.2.3 OCL algorithm**

For each local region  $V$  in  $I$ :

- a) compute the pixel-intensity gradient of  $V$  with centered differences method [Formulae (1), (2)];
- b) compute the covariance matrix  $C$  [Formula (6)];
- c) compute the eigenvalues of  $C$  to obtain  $Q_{\text{OCL}}^{\text{local}}$  [Formulae (11), (12), (13)].

Figure 2 visualizes the processing steps.



a) Current local region with the ratio between eigenvalues marked as ellipse

b) Local quality scores  $Q_{\text{OCL}}^{\text{local}}$  for example fingerprint image

**Figure 2 — Processing steps of orientation certainty level quality algorithm**

### 5.2.3 Local clarity score

#### 5.2.3.1 Description

Good quality fingerprints exhibit clear ridge-valley structure. Thus, the local clarity score (LCS) [4], which is the measure of the ridge-valley structure clarity, is a useful indicator of the quality of a fingerprint. The feature computes local quality and operates in a block-wise manner.

To perform ridge-valley structure analysis, the foreground of the finger image is quantised into local regions of size  $32 \times 32$  pixels [3]. Inside each local region, an orientation line, which is perpendicular to the ridge direction, is computed. At the centre of the local region along the ridge direction, a local region of size  $32 \times 16$  pixels shall be extracted and transformed to a vertically aligned local region.

On  $S$ , the local region average profile, calculated in 5.2.3.4, a linear regression (or least-square fitting) is applied to determine the Determine Threshold (DT) which is a line positioned at the centre of the local region  $V$ , and is used to segment the local region into the ridge or valley region. Regions with grey level intensity lower than DT are classified as ridges. Otherwise, they are classified as valleys.

Since good finger images cannot have ridges that are too close or too far apart, the nominal ridge and valley thickness can be used as a measure of the quality of the finger image captured. Similarly, ridges that are unreasonably thick or thin indicate that the finger image may not be captured properly, such as pressing too hard or too soft, or the image is a residual sample. Thus, the finger image quality can be determined by comparing the ridge and valley thickness to each of their nominal range of values. Any value out of the nominal range may imply a bad quality ridge pattern. To normalize the range of the thickness values, a pre-set maximum thickness is used. The maximum ridge or valley thickness ( $W_{\max}$ ) for a good finger image is estimated at 20 pixels for a 196,85 pixel per centimetre (500 pixel per inch). The pre-set value of 20 pixel for a 196,85 pixel per centimetre (500 pixel per inch) scanner spatial sampling rate is obtained from the median of the typical ridge separation of 8 to 12 pixels [1], and assuming that any ridge separation will not exceed twice of the median value. This will ensure that the pre-set value is indeed the maximum to limit the value of the normalized ridge and valley thickness between 0 and 1. The ridge thickness ( $W_r$ ) and valley thickness ( $W_v$ ) are then normalized with respect to the maximum thickness.

With the ridge and valley separated as above, a clarity test can be performed in each segmented rectangular 2-D region.

For local regions with good clarity, the pixel-intensity distribution of ridges and the pixel-intensity distribution of the valleys have a very small overlapping area and thus  $Q_{\text{LCS}}^{\text{local}}$  is high. The following factors affect the size of the total overlapping area:

- a) noise on ridge and valley;
- b) water patches on the image due to wet fingers;
- c) incorrect orientation angle due to the effect of directional noise;
- d) scar across the ridge pattern;
- e) highly curved ridges;
- f) ridge endings, bifurcations, delta and core points;
- g) incipient ridges, sweat pores and dots.

Factors a) to c) are physical noise found in the image. Factors d) to g) are actual physical characteristics of the fingerprint.

### 5.2.3.2 Computing the ridge valley signature of a local region

Given the local region  $V$  the ridge valley signature  $S$  is obtained by

$$s(x) = \frac{\sum_{y=1}^{16} V(x, y)}{16} \quad (14)$$

where  $V(x, y)$  is the grey level at point  $(x, y)$ ;  $x$  is the index along  $x$ -axis.

### 5.2.3.3 Determining the proportion of misclassified pixels

[Formulae \(15\)](#) and [\(16\)](#) specify the calculation of  $\alpha$  and which are the proportion of pixels misclassified respectively as valley or ridge.  $v_B$  is the number of pixels in valley region with intensity lower than DT and  $v_T$  is the total number of pixels in valley region.  $r_B$  is the number of pixels in the ridge region with intensity higher than DT and  $r_T$  is the total number of pixels in the ridge region.

$$\alpha = \frac{v_B}{v_T} \quad (15)$$

$$\beta = \frac{r_B}{r_T} \quad (16)$$

### 5.2.3.4 Determining the normalized ridge and valley width

The normalized valley width  $\bar{W}_v$  and the normalized ridge width  $\bar{W}_r$  are determined

$$\bar{W}_v = \frac{W_v}{\left(\frac{S}{125}\right) W^{\max}} \quad (17)$$

$$\bar{W}_r = \frac{W_r}{\left(\frac{S}{125}\right) W^{\max}} \quad (18)$$

where

$S$  is the scanner spatial sampling rate in dpi;

$W^{\max}$  is the estimated ridge or valley width for an image with 49,21 pixel per centimetre (125 pixel per inch) spatial sampling rate;

$W_v$  and  $W_r$  are the observed valley and ridge widths.

According to Reference [\[1\]](#),  $W^{\max} = 5$  is reasonable for 49,21 pixel per centimetre (125 pixel per inch) spatial sampling rate. By extension, the denominator in [Formula \(17\)](#) and the denominator in [Formula \(18\)](#) shall be 20 for a spatial sampling rate of 196,85 pixels per centimetre (500 pixels per inch).

### 5.2.3.5 Computing the local clarity score

The local quality score  $Q_{LCS}^{local}$  is the constrained average value of  $\alpha$  and  $\beta$  with a range between 0 and 1.

$$Q_{LCS}^{local} = \begin{cases} 1 - \frac{\alpha + \beta}{2}, & \text{if } (W_v^{nmin} < \bar{W}_v < W_v^{nmax}), (W_r^{nmin} < \bar{W}_r < W_r^{nmax}) \\ 0, & \text{otherwise} \end{cases} \quad (19)$$

where

$W_r^{nmin}$  and  $W_v^{nmin}$  are the minimum values for the normalized ridge and valley width;

$W_r^{nmax}$  and  $W_v^{nmax}$  are the maximum values for the normalized ridge and valley width.

$$W_r^{nmin} = \frac{3}{W_r} \quad (20)$$

$$W_r^{nmax} = \frac{10}{W_r} \quad (21)$$

$$W_v^{nmin} = \frac{2}{W_v} \quad (22)$$

$$W_v^{nmax} = \frac{10}{W_v} \quad (23)$$

NOTE Particular regions inherent in a fingerprint will negatively affect  $Q_{LCS}^{local}$ . For example, ridge endings and bifurcations or areas with high curvature such as those commonly found in core and delta points.

### 5.2.3.6 LCS algorithm

For each local region  $V$  in  $I$ :

- a) rotate  $V$  such that dominant ridge flow is perpendicular to x-axis;
- b) crop rotated  $V$  such that no invalid regions are included;
- c) with  $V$  obtain the ridge-valley signature  $S$  (5.2.3.2);
- d) determine DT using linear regression on  $S$ ;
- e) for each element  $S(x)$ , set threshold  $T(x)$  of  $x$  being ridge or valley based on DT;
- f) classify columns in  $V$  as ridge (1) or valley (0) with  $P(x) = \begin{cases} 1, & \text{if } S(x) < T(x); \\ 0, & \text{otherwise} \end{cases}$ ;
- g) determine ridge-valley transition vector  $C$  from  $P$ ;
- h) compute the vector  $W$  containing ridge and valley widths from  $C$ ;
- i) determine normalized ridge width and valley width  $\bar{W}_r$  and  $\bar{W}_v$  (5.2.3.4);
- j) determine the proportion of misclassified pixels  $\alpha$  and  $\beta$  (5.2.3.3);
- k) compute the local quality score  $Q_{LCS}^{local}$  (5.2.3.5).

Figure 3 visualizes the processing steps.

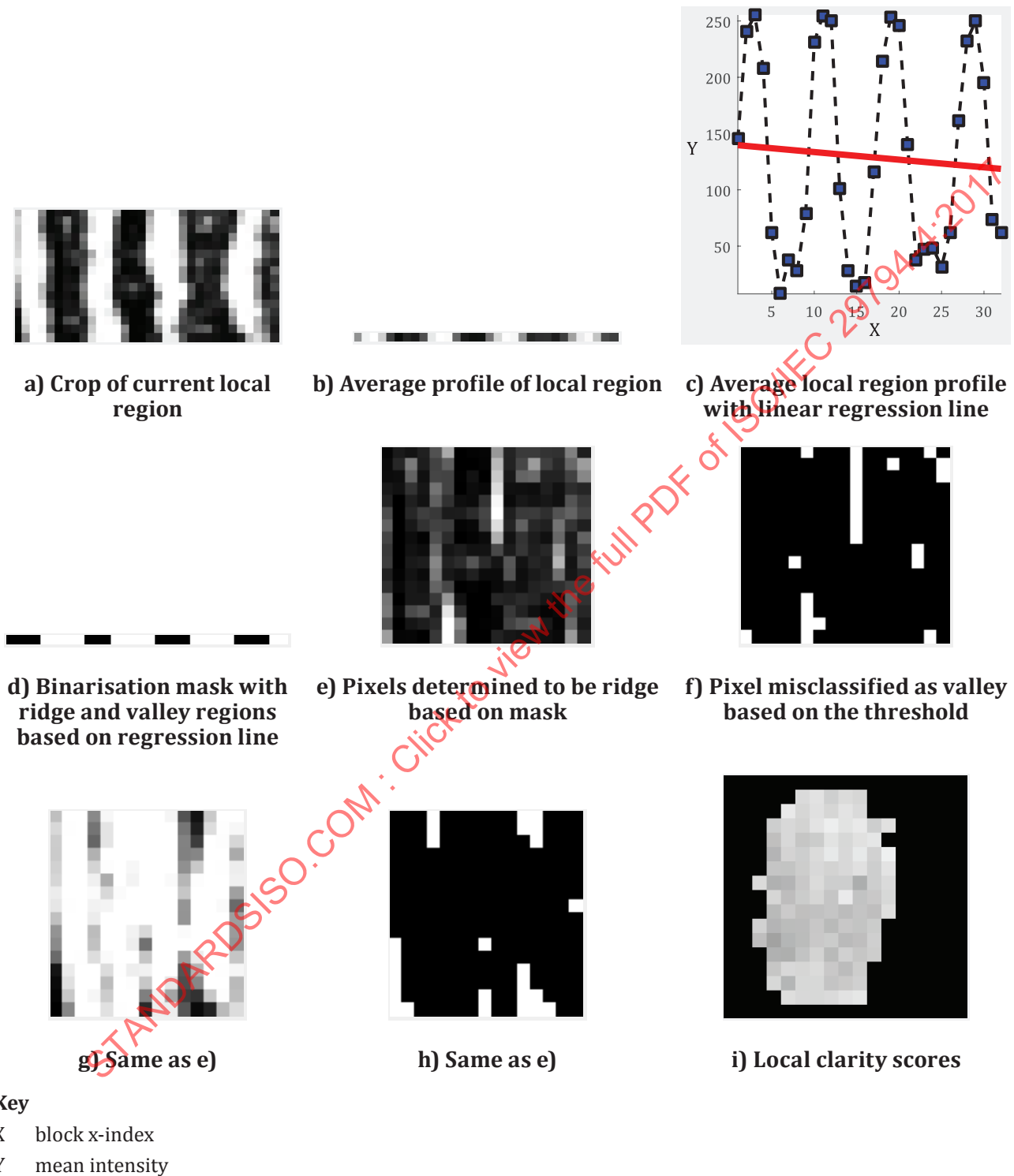


Figure 3 — Processing steps of local clarity score algorithm

## 5.2.4 Frequency domain analysis (FDA) score

### 5.2.4.1 Description

Frequency domain analysis (FDA) computes local quality and operates in a block-wise manner. A one-dimensional signature of the ridge-valley structure is extracted and the Discrete Fourier Transform (DFT) is computed on the signature to determine the frequency of the sinusoid following the ridge-valley structure<sup>[5]</sup>.

The ridge-valley signature of a high quality sample is a periodic signal, which can be approximated either by a square wave or a sinusoidal wave. In the frequency domain, an ideal square wave should exhibit a dominant frequency with sideband frequency components (sinc function). A sinusoidal wave consists of one dominant frequency and minimum components at other non-dominant frequencies.

For each local region, a signature perpendicular to the dominant ridge flow orientation is computed.

The FDA described in 5.2.4 computes the one-dimensional signatures by performing averaging along the ridge flow direction. The averaging process filters out noise along the ridge and valley flow and provides a modelling of a smooth changing signal in a direction perpendicular to ridge flow.

### 5.2.4.2 Computing the local FDA quality score

The local quality score is computed by using [Formula \(24\)](#):

$$Q_{FDA}^{local} = \begin{cases} 1, & \text{if } F_{max} = A_1 \text{ or } F_{max} = A_{|A|} \\ \frac{A_{F_{max}} + C(A_{F_{max-1}} + A_{F_{max+1}})}{\sum_{F=1}^{|A|/2} A_F}, & \text{otherwise} \end{cases} \quad (24)$$

where

$C$  is the attenuation parameter;

$A$  is the amplitude at frequency index  $x$ .

The value of  $Q_{FDA}^{local}$  is set to 1 when the maximum frequency  $F_{max}$  amplitude occurs at index  $F_{max} = A_1$  or  $F_{max} = A_{|A|}$ .

### 5.2.4.3 FDA algorithm

For each local region  $V$  in  $I$ :

- pad  $V$  with 2 pixel border;
- rotate  $V$  with nearest neighbour interpolation such that dominant ridge flow is perpendicular to x-axis;
- crop  $V$  such that no invalid regions are included;
- with  $V$  obtain the ridge-valley signature  $S$  (5.2.3.2);
- compute the DFT of  $S$  to obtain the magnitude representation  $A$ ;
- discard the first component of  $A$ ;
- determine  $F_{max}$  as the index with the largest magnitude in  $A$ ;
- compute  $Q_{FDA}^{local}$  of  $V$  using  $A$  and  $F_{max}$  (5.2.4.2).

Figure 4 visualizes the processing steps.

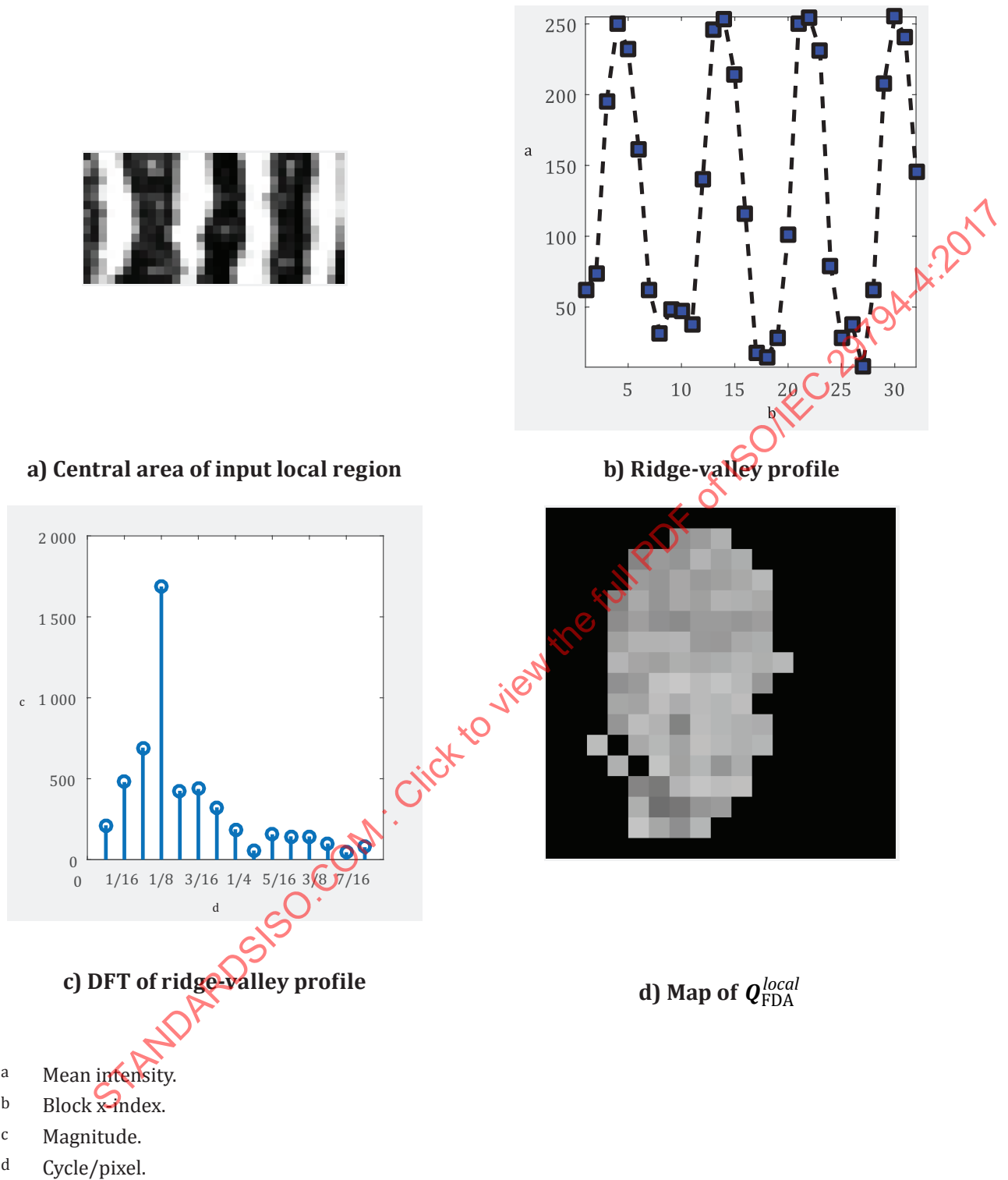


Figure 4 — Processing steps of FDA quality algorithm

## 5.2.5 Ridge valley uniformity

### 5.2.5.1 Feature description

Ridge valley uniformity (RVU) is a measure of the consistency of the ridge and valley widths[3]. The expectation for finger image with clear ridge and valley separation is that the ratio between ridge and valley widths remains fairly constant throughout the finger image.

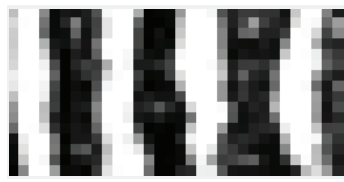
The ratio of ridge thickness to valley thickness should be constant and close to 1 throughout the whole image for a good quality finger image. The feature computes local quality and operates in a block-wise manner.

### 5.2.5.2 RVU algorithm

For each local region  $V$  in  $I$ :

- a) determine dominant ridgeflow orientation *angle* ( $V$ ) of  $V$ ;
- b) rotate  $V$  such that *angle* ( $V$ ) is perpendicular to x-axis;
- c) crop  $V$  such that no invalid regions are included;
- d) with  $V$  obtain the ridge-valley signature  $S$  (5.2.3.2);
- e) determine DT using linear regression on  $S$ ;
- f) for each  $S(x)$  compute threshold  $T(x) = x \times DT(1) + DT(0)$ ;
- g) binarize  $S$  using  $T$ ;
- h) classify ridge and valley in  $S$  as  $P(x) = \begin{cases} 1, & \text{if } S(x-1) < T(x), \\ 0, & \text{otherwise} \end{cases}$ ;
- i) compute ridge-valley transition vector as  $C(x) = \begin{cases} 1, & \text{if } P(x-1) \neq P(x) \\ 0, & \text{otherwise} \end{cases}$ ;
- j) Drop first and last transition from  $S$  using  $C$  to remove incomplete ridges or valleys and obtain  $S'$ ;
- k) Compute  $Q_{FDA}^{local}$  as the ratio between widths of ridge and valleys in  $S'$ .

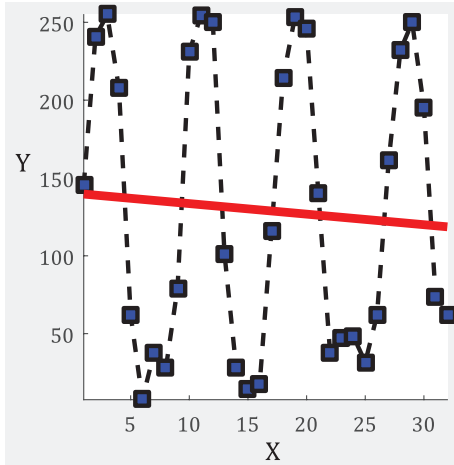
Figure 5 visualizes the processing steps.



a) Crop of current local region



b) Average profile of local region



c) Average profile with regression line



d) Local quality score as the standard deviation of local ridge to valley ratios

**Key**

- X block x-index
- Y mean intensity

**Figure 5 — Processing steps of ridge valley uniformity quality algorithm**

NOTE The ridge valley uniformity quality feature is spatial sampling rate dependent. The given defaults assume 196,85 pixel per centimetre (500 pixel per inch).

**5.2.6 Orientation flow**

**5.2.6.1 Description**

Orientation flow (OFL)<sup>[4]</sup> is a measure of ridge flow continuity which is based on the absolute orientation difference between a local region and its 8-neighborhood of local regions.

Orientation flow is a good indicator to describe the quality of a good fingerprint pattern because, in general, the flow of the ridge direction changes gradually, except in an area with a delta or a core. The feature computes local quality and operates in a block-wise manner.

**5.2.6.2 Local region-wise absolute orientation difference**

The ridge flow is determined as a measure of the absolute difference between a local region and its neighboring local regions. The absolute difference  $D(i, j)$  for local region  $V(i, j)$  is computed using the dominant ridge flow orientations of this local region and of its neighbors

$$D(i, j) = \frac{\sum_{m=-1}^1 \sum_{n=-1}^1 |angle(V(i, j)) - angle(V(i-m, j-n))|}{8} \tag{25}$$

### 5.2.6.3 Local orientation flow quality score

The local orientation quality score  $Q_{OFL}^{local}$  for the local region orientation difference  $D(i, j)$  is

$$Q_{OFL}^{local} = \begin{cases} \frac{D(i, j) - \theta_{\min}}{90^\circ - \theta_{\min}}, & \text{if } D(i, j) > \theta_{\min} \\ 0, & \text{otherwise} \end{cases} \quad (26)$$

where  $\theta_{\min} = 4$  is the threshold for minimum angle difference to consider.

### 5.2.6.4 OFL algorithm

- a) Determine the dominant ridge flow orientation *angle* ( $V$ ) of local region  $V$  in  $I$ .
- b) For each local region  $V$  in  $I$ :
  - 1) compute the absolute orientation difference  $D(i, j)$  using *angle* ( $V$ ) (5.2.6.2);
  - 2) compute the local orientation quality score  $Q_{OFL}^{local}$  (5.2.6.3).

Figure 6 visualizes the processing steps.

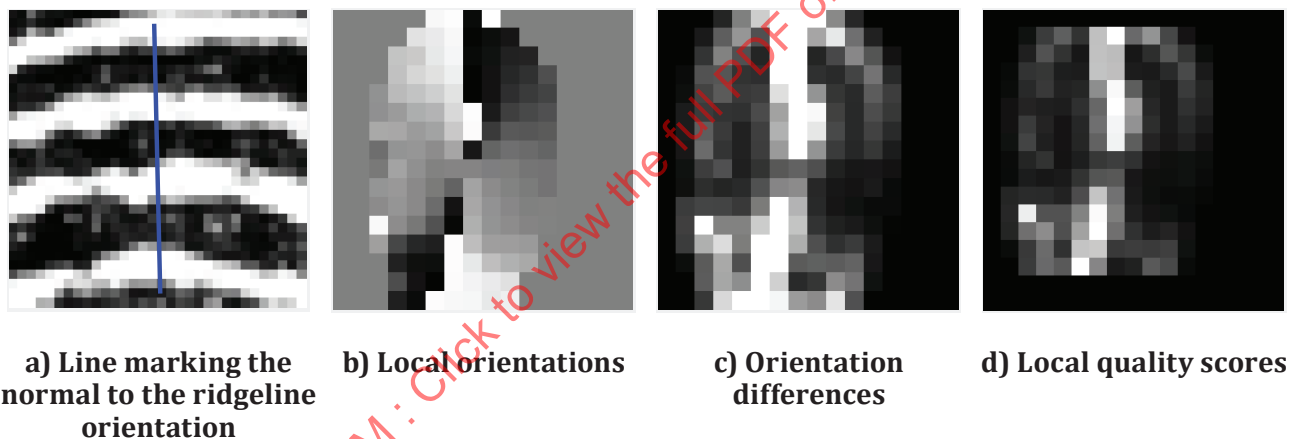


Figure 6 — Processing steps of orientation flow quality algorithm

## 5.2.7 MU

### 5.2.7.1 Description

The MU quality feature is the arithmetic mean of the pixel intensities of all pixels in the input image. The feature computes global quality.

### 5.2.7.2 MU algorithm

Compute  $Q_{MU}$  as the arithmetic mean of pixel intensities in  $I$ .

## 5.2.8 MMB

### 5.2.8.1 Description

The MMB quality feature is the arithmetic mean of per local region computed arithmetic mean in the gray scale input image. The feature computes local quality and operates in a block-wise manner.

### 5.2.8.2 MMB algorithm

- a) For each local region  $V$  in  $I$ 
  - 1) compute the arithmetic mean of the pixel intensities in  $V$  as  $Q_{MMB}^{local}$ .
- b) Compute  $Q_{MMB}$  as the arithmetic mean of set of  $Q_{MMB}^{local}$ .

## 5.2.9 Minutiae count in finger image

### 5.2.9.1 Description

The FingerJet FX (FJFX) minutiae extractor provides a count of detected minutiae in the finger image. The minutiae count has a bearing on the mated comparison score. The feature computes global quality.

### 5.2.9.2 MINCNT algorithm

$Q_{MIN}^{cnt}$  is the number of detected minutiae in the finger image as determined by FJFX.

## 5.2.10 Minutiae count in center of mass region

### 5.2.10.1 Description

The FingerJet FX (FJFX) minutiae extractor provides locations of detected minutiae in a finger image. The feature is the minutiae count in a  $200 \times 200$  pixels local region centered on the center of mass of the detected minutia. The feature computes local quality at the minutiae locations.

### 5.2.10.2 MINCOM algorithm

$Q_{MIN}^{com}$  is the number of minutiae occurring within a  $200 \times 200$  pixels local region centered at the center of mass of the locations of all detected minutiae in the finger image as determined by FJFX.

## 5.2.11 Minutiae quality based on local image mean

### 5.2.11.1 Description

The FingerJet FX (FJFX) minutiae extractor provides locations of detected minutiae in a finger image. For each minutia location a local quality based on image statistics is computed. The reported quality value is aggregated as the count of local qualities which occurs in the specified range. The feature computes local quality at the minutiae locations.

### 5.2.11.2 MINMU algorithm

$Q_{MIN}^{mu}$  is computed by first determining the local quality of each minutiae detected by FJFX as

$$Q_{MIN}^{local,mu} = \frac{\mu(I) - \mu(V)}{\sigma(I)} \quad (27)$$

where  $\mu(I)$  and  $\mu(V)$  is arithmetic mean of respectively the finger image and a  $32 \times 32$  pixels local region centered on the minutia and  $\sigma(I)$  is the standard deviation of the finger image.

The minutiae quality feature  $Q_{MIN}^{mu}$  is finally computed as the percentage of  $Q_{MIN}^{local\ mu}$  which have values between 0 and 0,5 as

$$Q_{MIN}^{mu} = \left| \left\{ (x, y) \mid 0 \leq Q_{MIN}^{local\ mu} < 0,5 \right\} \right|, \text{ for } 0 < i \leq Q_{MIN}^{cnt} \quad (28)$$

## 5.2.12 Minutiae quality based on local orientation certainty level

### 5.2.12.1 Description

The FingerJet FX (FJFX) minutiae extractor provides locations of detected minutiae in a finger image. For each minutia location a local orientation certainty level is computed. The reported quality value is aggregated as the count of local qualities which exceed the specified value. The feature computes local quality at the minutiae locations.

### 5.2.12.2 MIN<sup>OCL</sup> algorithm

$Q_{MIN}^{ocl}$  is computed by first determining the local quality of each minutiae detected by FJFX as

$$Q_{MIN}^{local\ ocl} = Q_{OCL}^{local}(\mathbf{V}) \quad (29)$$

where  $Q_{OCL}^{local}(\mathbf{V})$  is the local orientation certainty level (5.2.2) for the  $32 \times 32$  pixels local region  $\mathbf{V}$  centered on the minutia.

The minutiae quality feature  $Q_{MIN}^{ocl}$  is finally computed as the percentage of  $Q_{MIN}^{local\ ocl}$  which have values greater than 0,8 as

$$Q_{MIN}^{ocl} = \left| \left\{ (x, y) \mid Q_{MIN}^{local\ ocl} > 0,8 \right\} \right| \text{ for } 0 < i \leq Q_{MIN}^{cnt} \quad (30)$$

## 5.2.13 Region of interest image mean

### 5.2.13.1 Description

The region of interest for the finger image is the foreground region of the image containing the fingerprint. The mean image intensity in this area is computed over the set of  $32 \times 32$  pixels local regions which have a least one pixel contained in the region of interest. The feature computes global quality.

NOTE The quality score is highly correlated with  $Q_{MU}$  (5.2.7) and  $Q_{MMB}$  (5.2.8).

### 5.2.13.2 AREA algorithm

- a) Determine the region of interest  $\mathbf{R}$  (5.2.13.3).
- b) For each  $32 \times 32$  local region  $\mathbf{V}$  in  $\mathbf{I}$ 
  - 1) if  $\mathbf{V}$  has at least 1 pixel contained in foreground of  $\mathbf{R}$ , mark the local region as foreground.
- c) Compute  $Q_{AREA}^{\mu}$  as the arithmetic mean of the set of  $\mathbf{V}$  which are marked as foreground.

### 5.2.13.3 Determine the Region of Interest

- a) Erode the finger image  $\mathbf{I}$  with  $5 \times 5$  structuring element to obtain  $\mathbf{I}'$ .

- b) Apply normalized Gaussian blur filter (each weight is divided by the sum of all weights) with kernel size  $41 \times 41$  and standard deviation of 6,5 to  $I'$  to obtain  $G$ .
- c) Binarize  $G$  using Otsu's method<sup>[6]</sup> to obtain  $B$ .
- d) Apply normalized Gaussian blur filter (each weight is divided by the sum of all weights) with kernel size  $91 \times 91$  and standard deviation of 14,0 to  $B$  to obtain  $G'$ .
- e) Binarize  $G'$  using Otsu's method to obtain  $B'$ .
- f) Determine the contours of  $B'$  using Suzuki's method<sup>[7]</sup> to obtain  $C$ .
- g) Regions in  $C$  which are surrounded by 0 valued pixels shall be set to 0 valued pixels.
- h) 0 valued pixel regions in  $C$  which reach the image border but are not the largest area shall be set to 1 valued pixels.
- i) The resulting binary mask  $R$  contains the region of interest as a region of 0 valued pixels.

[Figure 7](#) visualizes the processing steps.

STANDARDSISO.COM : Click to view the full PDF of ISO/IEC 29794-4:2017

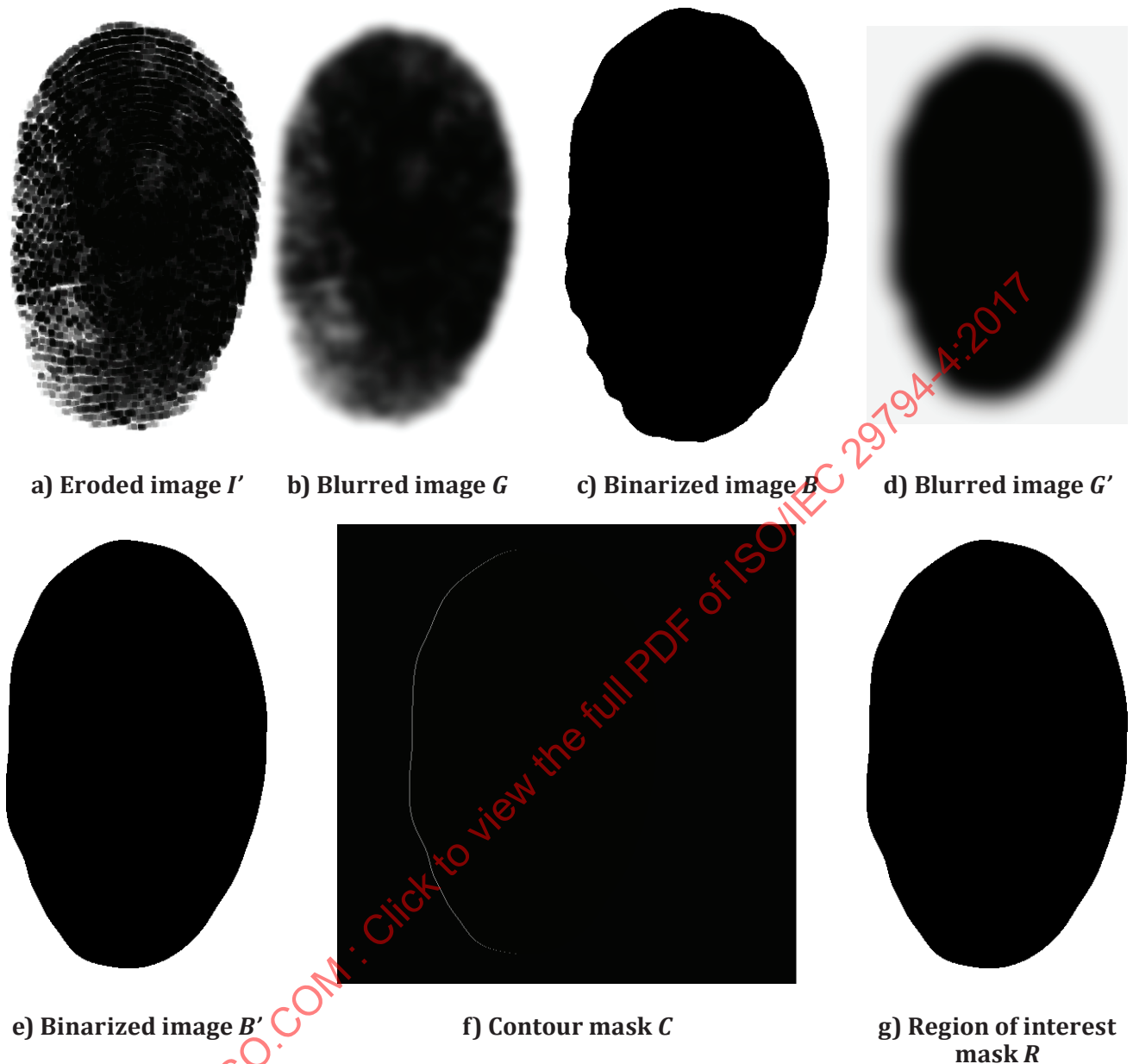


Figure 7 — Processing steps of region of interest algorithm

#### 5.2.14 Region of interest orientation map coherence sum

##### 5.2.14.1 Description

The orientation map coherence sum quantifies the coherence of the estimated finger image orientation field. The coherence map is computed according to coherence method specified in Reference [8]. The feature computes local quality and operates in a block-wise manner.

##### 5.2.14.2 COH<sup>SUM</sup> algorithm

- Compute the pixel-intensity gradient field  $\mathbf{g}$  of  $I$  (5.2.14.3).
- Compute the square gradient field as  $\mathbf{g}_s = (g_x^2 - g_y^2, 2g_x g_y)^T$ .
- Determine the region of interest  $\mathbf{R}$  (5.2.13.3).

- d) For each  $16 \times 16$  local region  $V$  in  $I$
- 1) if  $V$  has at least 1 pixel contained in foreground of  $R$ , compute the coherence of  $V$  as  $coh(V)(0)$ , otherwise set  $coh(V) = 0$ .
- e) Compute the quality score  $Q_{COH}^{sum}$  as the sum of the  $coh(V)$  of all  $V$ .

### 5.2.14.3 Computing the gradient field

The gradient field  $g = (g_x, g_y)^T$  of pixel intensity  $I(i, j)$  of  $I$  is

$$\begin{aligned} g_x(i, j) &= (I(i+1, j) - I(i-1, j)) / 2 \quad \text{for } 1 \leq i \leq I_w - 1, 0 \leq j \leq I_h \\ g_x(0, j) &= I(1, j) - I(0, j) \quad \text{for } 0 \leq j \leq I_h \\ g_x(I_w, j) &= I(I_w, j) - I(I_w - 1, j) \quad \text{for } 0 \leq j \leq I_h \end{aligned} \quad (31)$$

and

$$\begin{aligned} g_y(i, j) &= (I(i, j+1) - I(i, j-1)) / 2 \quad \text{for } 0 \leq i \leq I_w, 1 \leq j \leq I_h - 1 \\ g_y(i, 0) &= I(i, 1) - I(i, 0) \quad \text{for } 0 \leq i \leq I_w \\ g_y(i, I_h) &= I(i, I_h) - I(i, I_h - 1) \quad \text{for } 0 \leq i \leq I_w \end{aligned} \quad (32)$$

where  $I_w$  and  $I_h$  are respectively the width and height of  $I$  in pixels.

### 5.2.14.4 Computing the coherence of a local region

The coherence of a local region  $V$  is computed from its pixel-intensity gradient field  $g_s$  as

$$coh(V) = \frac{\left| \sum g_s(i, j) \right|}{\sum |g_s(i, j)|} \quad (33)$$

where  $|\cdot|$  denotes the Euclidean norm and the sums are taken over all pixels in  $V$ .

## 5.2.15 Region of interest relative orientation map coherence sum

### 5.2.15.1 Description

The relative orientation map coherence sum is the average of local region orientation coherence as determined by 5.2.14. The feature computes local quality and operates in a block-wise manner.

### 5.2.15.2 COHREL algorithm

- a) Compute  $Q_{COH}^{sum}$  and store the number of local regions  $V$  which have at least one pixel contained in  $R$  as  $n$  (5.2.14).
- b) Compute  $Q_{COH}^{rel} = \frac{Q_{COH}^{sum}}{n}$ .

## 5.2.16 Quality feature vector composition

### 5.2.16.1 Description

Quality features specified in 5.2.2 to 5.2.6 provide a map of values for local regions in the finger image. The quality features specified in 5.2.7 to 5.2.15 provide scalar quality values for the finger image.

The specified features shall be composed such that a fixed length feature vector is obtained for use by a classification system. Thus, the features in 5.2.2 to 5.2.6 are aggregated using arithmetic mean

specified in 5.2.16.2, standard deviation specified in 5.2.16.3 and histogram specified in 5.2.16.4 for inclusion in the final feature vector specified in 5.2.16.5.

### 5.2.16.2 Mean of local quality values

The mean quality value  $Q_{\text{AREA}}^{\mu}$  over an  $N \times M$  matrix of local quality values  $Q_{\text{QNAME}}^{\text{local}}$  is computed as

$$Q_{\text{QNAME}}^{\mu} = \frac{1}{N * M} \sum_{i=1}^N \sum_{j=1}^M Q_{\text{QNAME}}^{\text{local}} \quad (34)$$

where  $qname$  is one of OCL, LCS, FDA, RVU, OFL corresponding to the local quality values computed for orientation certainty (5.2.2), local clarity score (5.2.3), frequency domain analysis score (5.2.4), ridge valley uniformity (5.2.5), orientation flow (5.2.6).

This yields the arithmetic mean aggregated quality scores  $Q_{\text{OCL}}^{\mu}, Q_{\text{LCS}}^{\mu}, Q_{\text{FDA}}^{\mu}, Q_{\text{RVU}}^{\mu}, Q_{\text{OFL}}^{\mu}$

### 5.2.16.3 Standard deviation of local quality values

The standard deviation  $Q_{\text{QNAME}}^{\sigma}$  over an  $N \times M$  matrix of local quality values  $Q_{\text{QNAME}}^{\text{local}}$  is computed as

$$Q_{\text{QNAME}}^{\sigma} = \left( \frac{1}{N * M - 1} \sum_{i=1}^N \sum_{j=1}^M \left( Q_{\text{QNAME}}^{\text{local}}(i, j) - Q_{\text{QNAME}}^{\mu} \right)^2 \right)^{\frac{1}{2}} \quad (35)$$

where  $qname$  is one of OCL, LCS, FDA, RVU, OFL corresponding to the local quality values computed for orientation certainty (5.2.2), local clarity score (5.2.3), frequency domain analysis score (5.2.4), ridge valley uniformity (5.2.5), orientation flow (5.2.6).

This yields the standard deviation aggregated quality scores  $Q_{\text{OCL}}^{\sigma}, Q_{\text{LCS}}^{\sigma}, Q_{\text{FDA}}^{\sigma}, Q_{\text{RVU}}^{\sigma}, Q_{\text{OFL}}^{\sigma}$

### 5.2.16.4 Histogram of local quality

Local quality values from orientation certainty (5.2.2), local clarity score (5.2.3), frequency domain analysis score (5.2.4), ridge valley uniformity (5.2.5), orientation flow (5.2.6) shall be represented as fixed-length histograms with 10 bins to capture the distribution of local qualities.

The boundaries defining each bin for each of the features are specified as

$$\begin{aligned} B_{\text{FDA}} &= \{-\infty; 0,268\ 00; 0,304\ 00; 0,330\ 00; 0,355\ 00; \\ &\quad 0,380\ 00; 0,407\ 00; 0,440\ 00; 0,500\ 00; 1,000\ 00; \infty\} \\ B_{\text{LCS}} &= \{-\infty; 0,000\ 00; 0,700\ 00; 0,740\ 00; 0,770\ 00; \\ &\quad 0,790\ 00; 0,810\ 00; 0,830\ 00; 0,850\ 00; 0,870\ 00; \infty\} \\ B_{\text{OCL}} &= \{-\infty; 0,337\ 00; 0,479\ 00; 0,579\ 00; 0,655\ 00; \\ &\quad 0,716\ 00; 0,766\ 00; 0,810\ 00; 0,852\ 00; 0,898\ 00; \infty\} \\ B_{\text{OFL}} &= \{-\infty; 0,017\ 15; 0,035\ 00; 0,055\ 70; 0,081\ 00; \\ &\quad 0,115\ 00; 0,171\ 80; 0,256\ 90; 0,475\ 80; 0,748\ 00; \infty\} \end{aligned} \quad (36)$$

$$B_{RVU} = \{-\infty; 0,500\ 00; 0,667\ 00; 0,800\ 00; 1,000\ 00; 1,250\ 00; 1,500\ 00; 2,000\ 00; 24,000\ 0; 30,000\ 0; \infty\}$$

For each of FDA, LCS, OCL, OFL, RVU, a histogram is computed using the specified bin boundaries where the  $i$ th bin in the histogram is given by the interval

$$\begin{aligned} & (B_Q^i, B_Q^{i+1}) \quad , \text{for } 1=i \\ & [B_Q^i, B_Q^{i+1}) \quad , \text{for } 1 < i \leq |B_Q| \end{aligned} \tag{37}$$

The  $i$ th interval includes the value of  $B_Q^i$  on the left and excludes the value of  $B_Q^{i+1}$  on the right when  $1 < i \leq |B_Q|$ . In this document,  $|B_Q| = 10$ .

The histograms of local qualities are specified according to their bin boundaries as defined in [Formulae \(36\)](#) and [\(37\)](#) where the  $i$ th bin in the histogram contains the cardinality of the multiset that contains values bounded by the histogram boundaries

$$\begin{aligned} Q_{FDA}^i &= \left\{ (x, y) \mid B_{FDA}^i \leq \mathbf{Q}_{FDA}^{local} < B_{FDA}^{i+1} \right\} \quad , \text{for } 1 \leq i \leq |B_{FDA}|, \\ Q_{LCS}^i &= \left\{ (x, y) \mid B_{LCS}^i \leq \mathbf{Q}_{LCS}^{local} < B_{LCS}^{i+1} \right\} \quad , \text{for } 1 \leq i \leq |B_{LCS}|, \\ Q_{OCL}^i &= \left\{ (x, y) \mid B_{OCL}^i \leq \mathbf{Q}_{OCL}^{local} < B_{OCL}^{i+1} \right\} \quad , \text{for } 1 \leq i \leq |B_{OCL}|, \\ Q_{OFL}^i &= \left\{ (x, y) \mid B_{OFL}^i \leq \mathbf{Q}_{OFL}^{local} < B_{OFL}^{i+1} \right\} \quad , \text{for } 1 \leq i \leq |B_{OFL}|, \\ Q_{RVU}^i &= \left\{ (x, y) \mid B_{RVU}^i \leq \mathbf{Q}_{RVU}^{local} < B_{RVU}^{i+1} \right\} \quad , \text{for } 1 \leq i \leq |B_{RVU}|. \end{aligned} \tag{38}$$

The histogram for a single feature represented by its bins is written as

$$\mathbf{Q}_{QNAME} = \{Q_{QNAME}^i\}, \text{for } 1 \leq i \leq B_{QNAME} \tag{39}$$

where  $qname$  is one of OCL, LCS, FDA, RVU, OFL.

This yields the histogram feature vectors  $\mathbf{Q}_{OCL}, \mathbf{Q}_{LCS}, \mathbf{Q}_{FDA}, \mathbf{Q}_{RVU}, \mathbf{Q}_{OFL}$

### 5.2.16.5 ISO 29794-4 quality feature vector

This document's quality feature vector is specified as

$$\begin{aligned}
 Q_{29794-4} = \{ & Q_{OCL}^{\mu}, Q_{LCS}^{\mu}, Q_{FDA}^{\mu}, Q_{RVU}^{\mu}, Q_{OFL}^{\mu}, \\
 & Q_{OCL}^{\sigma}, Q_{LCS}^{\sigma}, Q_{FDA}^{\sigma}, Q_{RVU}^{\sigma}, Q_{OFL}^{\sigma}, \\
 & Q_{OCL}, Q_{LCS}, Q_{FDA}, Q_{RVU}, Q_{OFL}, \\
 & Q_{MU}, Q_{MMB}, Q_{COH}^{rel}, Q_{COH}^{sum}, Q_{AREA}^{\mu}, \\
 & Q_{MIN}^{cnt}, Q_{MIN}^{com}, Q_{MIN}^{\mu}, Q_{MIN}^{ocl} \}
 \end{aligned} \tag{40}$$

## 5.3 Non-normative quality metrics

### 5.3.1 General

[5.3](#) specifies non-normative finger image quality assessment algorithms.

### 5.3.2 Radial power spectrum

#### 5.3.2.1 Description

The radial power spectrum is a measure of maximal signal power in a defined frequency band of the global radial Fourier spectrum. Ridges can be locally approximated by means of a single sine wave, hence high energy concentration in a narrow frequency band corresponds to consistent ridge structures.

Since the ridges of a finger image can be locally approximated by one sine wave, large value of sine wave energy can represent the strong ridges. The robustness of the ridge structure can be used to measure the finger image quality.  $F$  is decided as the maximum Radial Fourier spectrum value within the reasonable Fourier domain. The reasonable Fourier domain refers to the region of neither the highest nor the lowest frequency. The higher the value of  $F$ , the better is the finger image quality.

#### 5.3.2.2 Variables

Name	Default	Description
$r_{min}$	0,143 cycles/pixel	Lower bound of frequency band
$r_{max}$	0,077 cycles/pixel	Upper bound of frequency band
$\Delta_r$		Sampling step between annular bands in the frequency spectrum
$\theta$	180	Degrees of the spectrum to consider

#### 5.3.2.3 Algorithm

- Compute the magnitude of the 2D-DFT  $F(u,v)$  of input image.
- Transform  $F(u,v)$  into polar coordinates and normalize to the range of [0, 1].
- Determine the maximum energy to compute  $Q_{POW}$  ([5.3.2.5](#)).

5.3.2.4 Magnitude of frequency bands polar coordinates

The magnitude of the annular band between  $r$  and  $r + \Delta_r$  in the polar Fourier spectrum  $F(\alpha,r)$  is computed as shown in Formula (41):

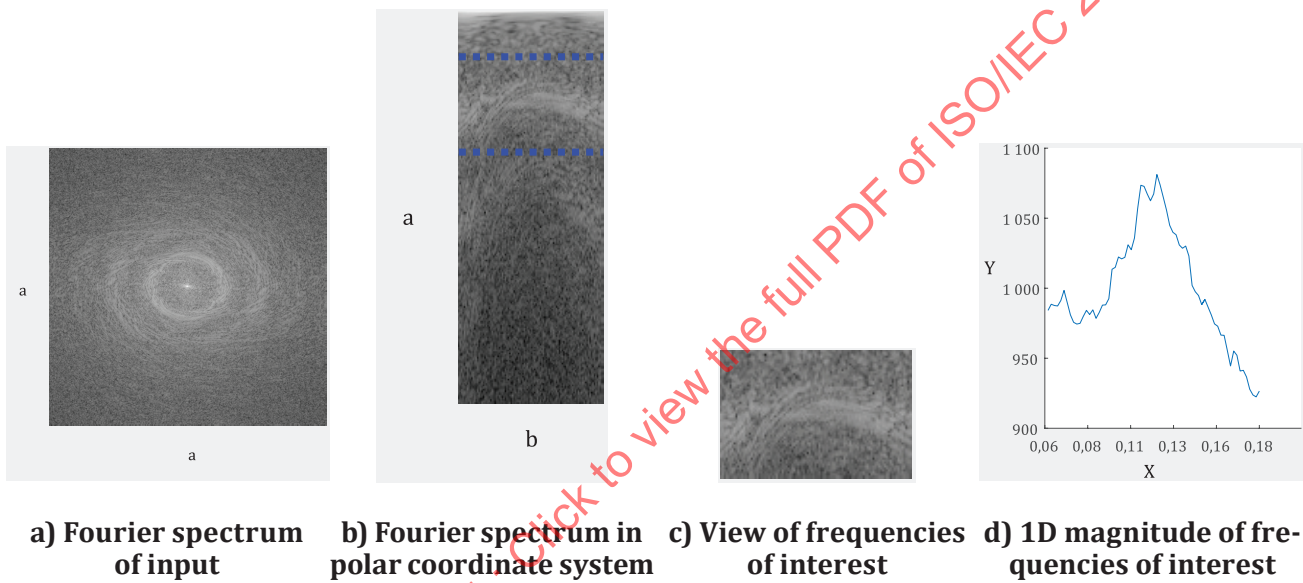
$$J(r) = \frac{\sum_{\alpha=0}^{\pi} \sum_r^{r+\Delta_r} F(\alpha,r)}{\sum_{\alpha=0}^{\pi} \sum_{r_{\min}}^{r_{\max}} F(\alpha,r)} \tag{41}$$

where

$\alpha$  is the angle;

$r$  is the radius.

$F(\alpha,r)$  is the Spectrum  $f(p,q)$  representation in polar coordinate system  $(\alpha,r)$ , see Figure 8.



Key

X cycles/pixel

Y magnitude

a Cycles/pixel.

b Radians.

Figure 8 — Processing steps of radial power spectrum algorithm

### 5.3.2.5 Determine quality score from energy distribution

The quality feature  $Q_{POW}$  is found as

$$Q_{POW} = \max_{r \in [\Delta r]} |J(r)| \quad (42)$$

NOTE The Radial Power Spectrum quality feature is spatial sampling rate dependent. The given defaults assume 196,85 pixel per centimetre (500 pixel per inch).

### 5.3.3 Gabor quality score

#### 5.3.3.1 Feature description

The Gabor quality feature operates on a per-pixel basis by calculating the standard deviation of the Gabor filter bank responses<sup>[9]</sup>. The size of the filter bank is used to determine a number of filters oriented evenly across the half circle. The strength of the response at a given location corresponds to the agreement between filter orientation and frequency in the location neighbourhood. For areas in the fingerprint image with a regular ridge-valley pattern there will be a high response from one or a few filter orientations. In areas containing background or unclear ridge-valley structure the Gabor response of all orientations will be low and constant.

#### 5.3.3.2 Variables

Name	Default	Description
$\sigma_x$	6	2D Gaussian standard deviation in x-direction
$\sigma_y$	6	2D Gaussian standard deviation in y-direction
$n$	4	Size of filter bank (orientations of the Gabor wave)
$f$	0,1	Gabor filter frequency
$\theta$	—	An orientation of a Gabor filter

#### 5.3.3.3 Algorithm

- Convolve input image with a 2D Gaussian kernel with  $\sigma=1$  and subtract it from the input image  $I$  to give  $\hat{I}$ .
- Compute the Gabor response of  $\hat{I}$  for each orientation  $\theta$ .
- Convolve the magnitude (complex modulus) of each Gabor response with a 2D Gaussian kernel with  $\sigma = 4$ .
- Compute the standard deviation of the Gabor magnitude response values at each location yielding a map of standard deviations.
- Sum the map of standard deviations and normalize according to number of sample points to produce the final Gabor quality score.

Figure 9 visualizes the processing steps.

5.3.3.4 Gabor filter

The general form of the complex 2D Gabor[10] filter  $h_{Cx}$  in the spatial domain is given by Formula (43):

$$h_{Cx}(x, y; f, \theta, \sigma_x, \sigma_y) = \exp\left(-\frac{1}{2}\left(\frac{x_\theta^2}{\sigma_x^2} + \frac{y_\theta^2}{\sigma_y^2}\right)\right) \exp(j2\pi fx_\theta) \tag{43}$$

where

$$x_\theta = x \sin \theta + y \cos \theta \tag{44}$$

$$y_\theta = x \cos \theta - y \sin \theta \tag{45}$$

and  $f$  is the frequency (cycles/pixel) of the sinusoidal plane wave along the orientation  $\theta$ . The size of the Gaussian smoothing window is determined by  $\sigma_x, \sigma_y$ .

The filter bank size  $n$  is used to compute the differently oriented Gabor filters composing the filter bank. Computing  $\theta$  given  $n$  is done as:

$$\theta = \frac{k-1}{n\pi}, k=1, \dots, n \tag{46}$$

NOTE The Gabor quality feature is spatial sampling rate dependent. The given defaults assume 196,85 pixel per centimetre (500 pixel per inch).

5.3.3.5 Computing the Gabor quality score from the Gabor filter response

Let  $G$  be a matrix with standard deviations of local responses resulting from convolution of  $I$  and Gabor filter of orientation  $n$ . The Gabor quality  $Q_{GAB}$  is computed as:

$$Q_{GAB} = \frac{1}{X*Y} \sum_x \sum_y G(x, y) \tag{47}$$

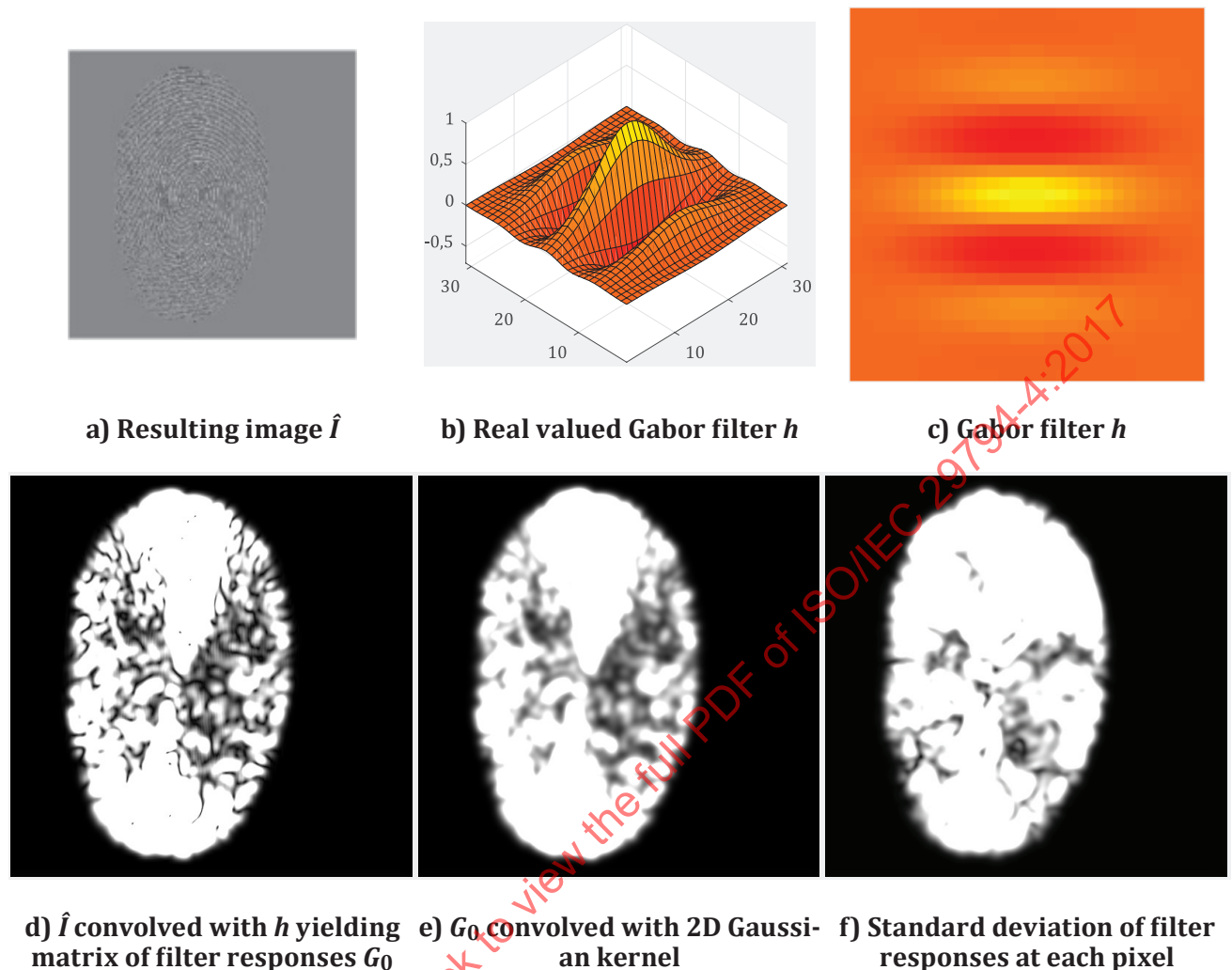


Figure 9 — Processing steps of Gabor algorithm

## 5.4 Unified quality score

### 5.4.1 Methodology for combining quality metrics

In order to obtain a single or unified output from several or all the quality metrics described in the earlier clauses, it is necessary to combine the values of the quality metrics described above and produce a single scalar quality score as required in the quality field. Each of the quality metrics shall be normalized to the range between 0 and 100 prior to combining them. Combining quality metrics shall be done such that the overall quality score is predictive of performance. There are various methods that can be used to combine all the quality metrics, e.g. weighted averaging, the use of pattern classifiers and other nonlinear computations.

### 5.4.2 Training method

Pattern classifiers are mathematical models that can intelligently learn a concept and predict an output when presented with new and even unseen samples. To apply pattern classification to combine the finger image quality analysis metrics, it is necessary to train the pattern classifier by providing finger images with the values for all the quality metrics computed and the overall quality scores for each sample. Once the pattern classifier is well-trained, given the values of the quality metrics, it will be able to provide an overall quality score for the finger image.

The feature vector,  $Q_{29794-4}$  (5.2.16.5), will be the input to the pattern classifier. Training the pattern classifier could be performed using a corpus of finger images with pre-assigned quality categories or scores such as the QSND corpus, on the output of one or many quality algorithms. A detailed approach to establish the QSND and the minimum number of samples required can be found in ISO/IEC 29794-1. For all the samples in the corpus, the feature vectors are computed. They are then paired with the quality category or score and fed into the pattern classifier for training.

With the feature vector specified in 5.2.16.5, a Random Forest shall be trained for binary classification, where Class 0 represents images of very low utility and Class 1 represents images of very high utility. The trained random forest outputs class membership along with its probability score. This score is the probability that a given image belongs to class 1 multiplied by 100 and rounded to its closest integer.

The number of images chosen for the training process shall conform to ISO/IEC 29794-1. The training set shall be chosen such that:

- a) Class 1 (or high utility) consists of images with NFIQ 1.0<sup>[11]</sup> value of 1 (with activation score >0,7) and genuine score in the 90<sup>th</sup> percentile for each of the comparison score providers.
- b) Class 0 (or low utility) consists of images with NFIQ 1.0 value of 5 (with activation score >0,9) and genuine score smaller than a threshold value that corresponds to false match rate of 1 in 10 000, i.e. false reject at false match rate of 0,000 1.

## 6 Finger image quality data record

### 6.1 Binary encoding

In binary data records, quality data shall be encoded as described in [Table 1](#).

Table 1 — Finger image quality data record structure

Byte #	Name	Length	Valid values	Description + Notes
0	Number of Quality Blocks	1 byte	0 to 255	This field is followed by the number of 5-byte Quality Blocks reflected by its value.  A value of zero (0) means that no attempt was made to assign a quality score. In this case, no Quality Blocks are present.
1	Quality score	1 byte	0 to 100, 255	Quality score of the metric identified by the Quality Algorithm Identifier (QAID) in bytes 4 and 5 of this Quality Block.  If quality score is equal to 255 (FF <sub>Hex</sub> ), an attempt to calculate a quality score has failed.
2-3	Quality Algorithm Vendor Identifier	2 bytes	0 to 65535 257 (0101 <sub>HEX</sub> ) for standard quality.	This field shall contain the identifier of the vendor whose algorithm was used to compute quality. Quality algorithm vendor identifier shall be registered with IBIA or other approved registration authority as a CBEFF biometric organization in accordance with CBEFF vendor ID registry procedures in ISO/IEC 19785-2. A value of all zeros shall indicate that the value for this field is unreported.  SC37 vendor ID (257 or 0101 <sub>HEX</sub> ) shall be used if and only if an SC 37 approved reference implementation is used to compute the quality score.  The reference implementation is posted at <a href="https://github.com/usnistgov/NFIQ2">https://github.com/usnistgov/NFIQ2</a> with the tag NFIQ2.0_29794-4_edition_2017.
4-5	Quality Algorithm Identifier (QAID)	2 bytes	1 to 65535	The quality algorithm identifier shall be encoded in two bytes. A value of all zeros is not permitted.  If encoding standard quality metrics defined in this document, the quality algorithm identifiers defined in <a href="#">Table 2</a> shall be used.  For encoding of quality components not defined in the specific modality parts the quality algorithm identifier shall be assigned by the vendor or an approved registration authority.
<b>Key</b> Byte 0: Record length Byte 1/2-3/4-5: 5-byte Quality Block [0 or more]				

Quality scores should always be placed within the quality record of the biometric data interchange record (BDIR) as defined in ISO/IEC 19794-x associated with the sample. CBEFF quality fields should not be used in place of 19794 quality fields but rather as supplementary data. The prescribed use of CBEFF quality fields may be supplied by each CBEFF patron format standard and is beyond the scope of this document. Multiple quality scores calculated by the same algorithm (same quality algorithm vendor identifier and same quality algorithm identifier) shall not be present in a single BDIR.

## 6.2 XML encoding

In XML documents, quality data shall be encoded as described in the following XML type definitions.

```
<xs:complexType name="RegistryIDType">
  <xs:sequence>
    <xs:element name="Organization" type="xs:unsignedShort"/>
    <xs:element name="Identifier" type="xs:unsignedShort"/>
  </xs:sequence>
</xs:complexType>

<xs:complexType name="QualityListType">
  <xs:sequence>
```

```

    <xs:element name="Quality" type="QualityType" maxOccurs="255"/>
  </xs:sequence>
</xs:complexType>

<xs:complexType name="QualityType">
  <xs:sequence>
    <xs:element name="Algorithm" type="RegistryIDType"/>
    <xs:choice>
      <xs:element name="Score" type="QualityScoreType"/>
      <xs:element name="QualityCalculationFailed">
        <xs:complexType/>
      </xs:element>
    </xs:choice>
  </xs:sequence>
</xs:complexType>

<xs:simpleType name="QualityScoreType">
  <xs:restriction base="xs:unsignedByte">
    <xs:minInclusive value="0"/>
    <xs:maxInclusive value="100"/>
  </xs:restriction>
</xs:simpleType>

```

### 6.3 Quality algorithm identifiers

The owner of the quality algorithms defined in this document is ISO/IEC JTC 1/SC 37. Its organization identifier is 257 (101Hex). [Table 2](#) lists the quality algorithm identifiers for the quality metrics defined in this document.

If a unified quality score is calculated and reported in a finger image quality data record, the normative quality metrics defined in [5.2](#) have to be calculated first. The values of the normative quality metrics defined in [5.2](#) may but need not be reported in the finger image quality data record. Calculation and reporting of the non-normative quality metrics defined in [5.3](#) is optional.

NOTE The unified quality score consists of the features in [Formula \(41\)](#) in [5.2.16.5](#).

**Table 2 — Quality metric identifier**

Quality algorithm identifier Hex	Quality algorithm identifier decimal	Quality metric	Algorithm feature name	Governing subclause + description
01Hex	01	Unified quality score ( $Q_{29794-4}$ )		Finger image quality score ( <a href="#">5.4</a> )
02Hex	02	Mean of local orientation certainty level ( $Q_{OCL}^{\mu}$ )	OCL	<a href="#">5.2.2</a> , <a href="#">5.2.16.2</a>
03Hex	03	Standard deviation of local orientation certainty level ( $Q_{OCL}^{\sigma}$ )	OCL	<a href="#">5.2.2</a> , <a href="#">5.2.16.3</a>
04Hex	04	Mean of local clarity score ( $Q_{LCS}^{\mu}$ )	LCS	<a href="#">5.2.3</a> , <a href="#">5.2.16.2</a>
05Hex	05	Standard deviation of local clarity score ( $Q_{LCS}^{\sigma}$ )	LCS	<a href="#">5.2.3</a> , <a href="#">5.2.16.3</a>
06Hex	06	Mean of local frequency domain analysis ( $Q_{FDA}^{\mu}$ )	FDA	<a href="#">5.2.4</a> , <a href="#">5.2.16.2</a>
07Hex	07	Standard deviation of local frequency domain analysis ( $Q_{FDA}^{\sigma}$ )	FDA	<a href="#">5.2.4</a> , <a href="#">5.2.16.3</a>
08Hex	08	Mean of local ridge valley uniformity ( $Q_{RVU}^{\mu}$ )	RVU	<a href="#">5.2.5</a> , <a href="#">5.2.16.2</a>
09Hex	09	Standard deviation of local ridge valley uniformity ( $Q_{RVU}^{\sigma}$ )	RVU	<a href="#">5.2.5</a> , <a href="#">5.2.16.3</a>
0AHex	10	Mean of local orientation flow ( $Q_{OFL}^{\mu}$ )	OFL	<a href="#">5.2.6</a> , <a href="#">5.2.16.2</a>

Table 2 (continued)

Quality algorithm identifier Hex	Quality algorithm identifier decimal	Quality metric	Algorithm feature name	Governing subclause + description
0B <sub>Hex</sub>	11	Standard deviation of orientation flow ( $Q_{OFL}^{\sigma}$ )	OFL	<a href="#">5.2.6</a> , <a href="#">5.2.16.3</a>
0C <sub>Hex</sub>	12	MU ( $Q_{MU}$ )	MU	<a href="#">5.2.7</a>
0D <sub>Hex</sub>	13	MMB ( $Q_{MMB}$ )	MMB	<a href="#">5.2.8</a>
0E <sub>Hex</sub>	14	Minutiae count ( $Q_{MIN}^{cnt}$ )	MIN <sup>CNT</sup>	<a href="#">5.2.9</a>
0F <sub>Hex</sub>	15	Minutiae count in center of mass ( $Q_{MIN}^{com}$ )	MIN <sup>COM</sup>	<a href="#">5.2.10</a>
10 <sub>Hex</sub>	16	Minutiae quality based on image mean ( $Q_{MIN}^{mu}$ )	MIN <sup>MU</sup>	<a href="#">5.2.11</a>
11 <sub>Hex</sub>	17	Minutiae quality based on orientation certainty level ( $Q_{MIN}^{ocl}$ )	MIN <sup>OCL</sup>	<a href="#">5.2.12</a>
12 <sub>Hex</sub>	18	Region of interest image mean ( $Q_{AREA}^{\mu}$ )	AREA	<a href="#">5.2.13</a>
13 <sub>Hex</sub>	19	Region of interest orientation map coherence sum ( $Q_{COH}^{sum}$ )	COH <sup>SUM</sup>	<a href="#">5.2.14</a>
14 <sub>Hex</sub>	20	Region of interest relative orientation map coherence sum ( $Q_{COH}^{rel}$ )	COH <sup>REL</sup>	<a href="#">5.2.15</a>
15 <sub>Hex</sub>	21	Radial power spectrum ( $Q_{POW}$ )	POW	<a href="#">5.3.2</a>
16 <sub>Hex</sub>	22	Gabor quality score ( $Q_{GAB}$ )	GAB	<a href="#">5.3.3</a>

## Annex A (normative)

### Conformance test assertions

#### A.1 Overview

This document specifies terms and quantitative methodologies relevant to characterizing the quality of finger images and to assessing their potential for high confidence biometric match decisions.

The objective of this document cannot be completely achieved until biometric products can be tested to determine whether they conform to those specifications. Conforming implementations are a necessary prerequisite for achieving interoperability among implementations; therefore there is a need for a standardised conformance testing methodology, test assertions, and test procedures as applicable to specific modalities addressed by this document. The test assertions will cover as much as practical of this document's requirements (covering the most critical features), so that the conformity results produced by the test suites will reflect the real degree of conformity of the implementations to ISO/IEC 29794-4 finger image quality data records. This is the motivation for the development of this conformance testing methodology.

This annex is intended to specify elements of conformance testing methodology, test assertions, and test procedures as applicable to this document.

#### A.2 Conformance test set

To verify conformance, implementations of quality assessment algorithms claiming conformance with this document should run on all images in the conformance test set. In order to conform, no output value shall differ from that of the reference implementation by more than 1 %.

The finger images in the conformance test set are selected from databases DB1 and DB3 of FVC2000<sup>[12]</sup> and database DB1 of FVC2002<sup>[13]</sup>.

NFIQ 2.0, the source code of which is available from <https://github.com/usnistgov/NFIQ2> is the reference implementation for this document.

Table A.1 — Quality metric values for conformance test set

Image identifier	$Q_{29794-4}$	$(Q_{OCL}^{\mu})$	$Q_{OCL}^{\sigma}$	$(Q_{LCS}^{\mu})$	$Q_{LCS}^{\sigma}$	$(Q_{FDA}^{\mu})$	$Q_{FDA}^{\sigma}$	$(Q_{RVU}^{\mu})$	$Q_{RVU}^{\sigma}$	$(Q_{OFL}^{\mu})$	$Q_{OFL}^{\sigma}$	$Q_{MU}$	$Q_{MMB}$	$Q_{MIN}^{cnt}$	$Q_{MIN}^{com}$	$Q_{MIN}^{mu}$	$Q_{MIN}^{ocl}$	$(Q_{AREA}^{\mu})$	$Q_{COH}^{sum}$	$Q_{COH}^{rel}$
FVC2000/ Db3/25_3	91	0,717 89	0,178 6	0,779 2	0,209 74	0,464 1	0,175 51	1,146 5	0,676 02	0,206 1	0,330 77	162,85	162,71	65	25	0,769 23	0,292 31	141,88	429,13	0,627 39
FVC2002/ Db1/49_6	89	0,699 26	0,152 1	0,749 95	0,213 63	0,420 52	0,146 2	1,087 9	0,644 27	0,184 48	0,249 32	213,76	214,45	50	30	0,38	0,26	189,8	177,01	0,567 33
FVC2002/ Db1/51_4	88	0,720 02	0,186 92	0,700 78	0,279 7	0,397 74	0,134 41	1,058 5	0,645 33	0,276 58	0,370 71	216,56	218,21	73	43	0,479 45	0,369 86	193,68	179,39	0,614 34
FVC2002/ Db1/89_1	88	0,759 1	0,125 64	0,775 16	0,184 25	0,432 01	0,128 75	1,048 6	0,381 94	0,165 16	0,257 04	206,52	209,58	47	33	0,212 77	0,361 7	187,89	230,78	0,635 76
FVC2000/ Db3/108_3	87	0,700 7	0,181 21	0,766 59	0,198 41	0,463 26	0,202 26	1,143 4	0,765 68	0,208 76	0,301 76	171,2	171,1	108	35	0,611 11	0,203 7	150,28	399,33	0,596 01
FVC2000/ Db3/108_4	87	0,714 75	0,159 09	0,763 39	0,213 69	0,462 27	0,190 49	1,115 4	0,606 46	0,176 14	0,256 31	171,0	170,93	103	38	0,669 9	0,213 59	154,88	425,99	0,603 39
FVC2000/ Db1/69_6	86	0,790 2	0,131 67	0,776 39	0,184 42	0,418 15	0,159 72	1,124 9	0,483 43	0,177 73	0,246 82	200,44	202,69	34	30	0,558 82	0,588 24	196,39	212,86	0,673 59
FVC2000/ Db3/26_2	86	0,647 79	0,227 93	0,767 41	0,216 76	0,496 57	0,227 53	1,099 8	0,839 79	0,220 35	0,326 13	184,81	184,83	83	28	0,698 8	0,096 386	158,29	317,28	0,539 58
FVC2000/ Db3/24_4	85	0,641 96	0,247 58	0,793 79	0,157 17	0,458 02	0,155 46	1,118 7	0,919 16	0,228 53	0,314 37	197,72	197,69	66	36	0,727 27	0,136 36	163,87	290,62	0,564 31
FVC2002/ Db1/29_2	85	0,757 01	0,164 81	0,677 2	0,311 73	0,407 91	0,122 01	1,142 2	0,676 79	0,156 83	0,252 77	219,83	221,24	40	25	0,4	0,5	196,26	195,07	0,686 86
FVC2002/ Db1/51_5	84	0,837 87	0,113 31	0,760 87	0,228 51	0,409 84	0,138 23	1,186 7	0,707 45	0,182 64	0,254 32	183,61	186,89	62	38	0,354 84	0,516 13	152,12	264,94	0,731 87
FVC2002/ Db1/55_6	84	0,803 25	0,186 33	0,758 03	0,247 98	0,423 25	0,168 39	1,146 1	0,631 1	0,262 18	0,346 74	179,95	186,56	44	30	0,25	0,613 64	145,32	225,59	0,723 06
FVC2002/ Db1/110_7	83	0,698 28	0,167 72	0,812 61	0,105 57	0,438 18	0,114 51	1,034 9	0,368 8	0,257 66	0,375 16	202,51	204,65	43	30	0,348 84	0,162 79	184,12	220,45	0,574 09
FVC2002/ Db1/14_6	83	0,809 43	0,179 87	0,831 77	0,110 47	0,421 29	0,146 4	1,040 9	0,456 23	0,181 92	0,267 92	180,28	183,31	43	24	0,395 35	0,674 42	139,95	261,83	0,793 42
FVC2000/ Db1/69_8	82	0,755 95	0,158 07	0,719 38	0,246 85	0,418 4	0,197 32	1,205 3	1,008 4	0,200 34	0,268 21	204,55	206,81	39	33	0,615 38	0,487 18	199,99	204,03	0,651 84
FVC2000/ Db3/108_6	82	0,630 43	0,164 31	0,726 3	0,233 68	0,473 02	0,213 12	1,139 3	0,896 06	0,214 18	0,295 98	156,11	155,97	94	29	0,606 38	0,053 191	143,92	364,03	0,508 43
FVC2002/ Db1/105_2	81	0,735 71	0,157 95	0,755 97	0,209 53	0,418 05	0,120 32	1,09	0,602 76	0,152 8	0,225 44	219,97	221,93	45	25	0,533 33	0,422 22	204,37	216,13	0,633 82
FVC2002/ Db1/106_5	81	0,841 79	0,125 26	0,773 5	0,224 91	0,410 14	0,162 75	1,205 1	0,952 16	0,129 99	0,231 47	177,99	181,45	47	22	0,340 43	0,595 74	147,05	275,5	0,752 73
FVC2000/ Db1/36_6	80	0,831 35	0,131 13	0,778 45	0,207 26	0,451 44	0,207 01	1,085 3	0,575 92	0,203 5	0,281 85	179,08	182,44	49	37	0,346 94	0,734 69	167,09	212,57	0,778 66

Table A.1 (continued)

Image identifier	$Q_{29794-4}$	$(Q_{OCL}^{\mu})$	$Q_{OCL}^{\sigma}$	$(Q_{LCS}^{\mu})$	$Q_{LCS}^{\sigma}$	$(Q_{FDA}^{\mu})$	$Q_{FDA}^{\sigma}$	$(Q_{RVU}^{\mu})$	$Q_{RVU}^{\sigma}$	$(Q_{OFL}^{\mu})$	$Q_{OFL}^{\sigma}$	$Q_{\mu}$	$Q_{MMB}$	$Q_{MIN}^{cnt}$	$Q_{MIN}^{com}$	$Q_{MIN}^{\mu}$	$Q_{MIN}^{ocl}$	$(Q_{AREA}^{\mu})$	$Q_{COH}^{sum}$	$Q_{COH}^{rel}$
FVC2000/ Db1/9_5	80	0,811 21	0,125 11	0,821 3	0,143 14	0,452 29	0,170 87	1,089 87	0,579 58	0,155 38	0,217 22	196,62	197,49	30	22	0,566 67	0,6	186,48	187,91	0,776 5
FVC2000/ Db1/104_8	79	0,814 04	0,147 77	0,772 07	0,203 87	0,473 6	0,208 54	1,031 5	0,452 82	0,180 95	0,255 84	190,08	191,78	41	29	0,390 24	0,512 2	183,02	220,54	0,768 42
FVC2000/ Db1/69_5	79	0,801 31	0,124 32	0,780 8	0,161 07	0,422 37	0,182 3	1,156 3	0,757 61	0,189 6	0,263 2	195,53	197,64	47	37	0,276 6	0,382 98	186,23	179,45	0,714 96
FVC2000/ Db1/28_5	78	0,813 88	0,139 9	0,681 26	0,346 17	0,498 83	0,242 17	1,102 9	0,693 11	0,212 73	0,283 81	182,41	186,25	48	35	0,333 33	0,687 5	167,7	183,75	0,775 33
FVC2000/ Db1/58_6	78	0,756 28	0,183 44	0,710 23	0,258 96	0,495 03	0,275 31	1,266 8	1,168 6	0,181 53	0,247 27	205,88	207,93	25	25	0,32	0,64	196,84	184,96	0,719 7
FVC2000/ Db1/28_6	77	0,835 49	0,128 01	0,717 55	0,287 96	0,474 42	0,228 28	1,162 1	1,046 6	0,185 48	0,266 1	183,69	187,12	44	36	0,227 27	0,772 73	170,39	194,9	0,808 73
FVC2000/ Db1/33_1	77	0,729 08	0,183 7	0,666 11	0,283 54	0,473 9	0,261 58	1,222 7	1,255 55	0,213 76	0,251 06	210,21	211,58	24	24	0,375	0,291 67	200,91	156,18	0,697 23
FVC2000/ Db1/11_5	76	0,817 94	0,124 6	0,765 79	0,204 26	0,526 56	0,273 01	1,155 1	0,809 55	0,190 32	0,273 88	180,84	184,67	24	17	0,166 67	0,541 67	166,97	205,04	0,740 21
FVC2000/ Db1/19_5	76	0,662 7	0,269 2	0,653 68	0,293 43	0,475 78	0,283 17	1,250 7	1,121 6	0,221 94	0,250 11	228,96	229,7	20	20	0,35	0,45	220,45	165,7	0,696 22
FVC2000/ Db1/104_6	75	0,833	0,118 97	0,793 94	0,187 49	0,487 62	0,240 15	1,211 1	1,053 01	0,206 66	0,307 01	190,83	192,94	34	25	0,470 59	0,588 24	181,09	218,74	0,762 16
FVC2000/ Db1/105_3	75	0,775 3	0,175 58	0,750 15	0,228 5	0,506 13	0,251 08	1,142 3	0,891 74	0,275 98	0,403 61	166,07	170,75	36	28	0,361 11	0,611 11	148,8	195,82	0,701 86
FVC2000/ Db1/2_5	74	0,854 55	0,109 76	0,749 56	0,254 97	0,503 3	0,245 8	1,087 5	0,645 79	0,146 59	0,235 06	183,05	185,21	41	32	0,609 76	0,682 93	173,2	230,12	0,810 28
FVC2000/ Db1/24_5	74	0,768 12	0,169 94	0,737 03	0,248 89	0,485 48	0,241 05	1,161 5	0,762 78	0,234 67	0,317 8	189,4	193,37	32	28	0,281 25	0,625	178,67	197,27	0,702 01
FVC2000/ Db1/25_8	73	0,802 28	0,170 56	0,722 49	0,261 25	0,525 34	0,282 34	1,165 6	0,981 6	0,188 63	0,234 21	196,68	199,61	51	43	0,196 08	0,588 24	185,73	211,96	0,765 2
FVC2000/ Db1/28_2	73	0,773 35	0,164 93	0,711 48	0,272 02	0,484 68	0,249 03	1,154 1	0,905 61	0,178 3	0,244 23	188,11	190,13	34	33	0,323 53	0,705 88	175,41	186,8	0,741 29
FVC2000/ Db1/101_7	72	0,856 26	0,089 989	0,814 62	0,165 71	0,466 62	0,207 64	1,115 2	0,664 97	0,155 16	0,239 95	181,75	184,1	26	17	0,307 69	0,692 31	176,86	252,17	0,778 31
FVC2000/ Db1/101_8	72	0,851 78	0,117 62	0,831 4	0,141 55	0,458 87	0,178 08	1,192 8	0,747 95	0,194 13	0,304 35	190,73	193,14	16	8	0,625	0,812 5	181,17	238,19	0,796 61
FVC2000/ Db1/20_6	71	0,809 84	0,142 7	0,750 24	0,219 04	0,467 91	0,224 06	1,195 5	0,925 74	0,141 76	0,218 9	187,25	189,45	36	29	0,333 33	0,5	175,13	183,67	0,784 92
FVC2000/ Db1/23_2	71	0,815 22	0,141 62	0,808 06	0,105 99	0,529 64	0,250 16	1,147 2	0,890 58	0,142	0,204 89	190,06	193,46	30	25	0,366 67	0,566 67	174,57	175,27	0,793 09

Table A.1 (continued)

Image identifier	$Q_{29794-4}$	$(Q_{OCL}^{\mu})$	$Q_{OCL}^{\sigma}$	$(Q_{LCS}^{\mu})$	$Q_{LCS}^{\sigma}$	$(Q_{FDA}^{\mu})$	$Q_{FDA}^{\sigma}$	$(Q_{RVU}^{\mu})$	$Q_{RVU}^{\sigma}$	$(Q_{OFL}^{\mu})$	$Q_{OFL}^{\sigma}$	$Q_{MU}$	$Q_{MMB}$	$Q_{MIN}^{cnt}$	$Q_{MIN}^{com}$	$Q_{MIN}^{mu}$	$Q_{MIN}^{ocl}$	$(Q_{AREA}^{\mu})$	$Q_{COH}^{sum}$	$Q_{COH}^{rel}$
FVC2000/ Db1/101_1	70	0,840 93	0,117 8	0,881 37	0,144 52	0,499 93	0,223 86	1,173 7	1,089 9	0,212 63	0,348 09	178,11	180,99	16	12	0,5	0,687 5	158,7	187,32	0,800 51
FVC2000/ Db1/16_5	70	0,801 14	0,159 58	0,758 87	0,242 47	0,530 63	0,265 72	1,061 1	0,522 09	0,165 7	0,240 58	196,99	198,7	37	32	0,405 41	0,594 59	186,85	202,14	0,780 46
FVC2000/ Db1/101_6	69	0,869 15	0,082 228	0,829 97	0,139 11	0,489 74	0,182 88	1,014 4	0,512 75	0,169 53	0,280 37	185,06	187,51	23	15	0,173 91	0,652 17	176,03	231,33	0,806 02
FVC2000/ Db1/105_8	69	0,824 5	0,146 93	0,816 12	0,139 74	0,532 1	0,279 18	1,114 2	0,639 81	0,160 46	0,252 41	197,93	201,16	25	21	0,2	0,68	182,51	213,97	0,783 79
FVC2000/ Db1/102_5	68	0,783 23	0,182 28	0,630 49	0,331 37	0,447 54	0,249 19	1,150 4	0,912 19	0,174 77	0,242 17	193,02	194,88	42	36	0,309 52	0,476 19	181,55	186,9	0,765 98
FVC2000/ Db1/104_3	68	0,771 97	0,137 38	0,752 24	0,200 25	0,480 15	0,242 31	1,161 6	0,868 49	0,178 38	0,263 31	218,62	220,08	38	29	0,5	0,394 74	212,88	172,96	0,686 36
FVC2000/ Db1/101_5	67	0,852 87	0,089 017	0,822 36	0,168 17	0,515 43	0,223 5	1,154 2	0,732 45	0,197 54	0,280 35	185,09	188,23	19	14	0,421 05	0,789 47	173,13	224,86	0,780 75
FVC2000/ Db1/103_4	67	0,789 73	0,131 76	0,718 98	0,267 83	0,533 38	0,280 88	1,138 9	0,749 48	0,166 01	0,231 7	197,7	200,45	34	31	0,205 88	0,411 76	188,08	184,99	0,703 38
FVC2000/ Db1/101_2	66	0,856 63	0,097 301	0,832 07	0,141 78	0,489 96	0,193 15	1,078	0,495 31	0,182 97	0,273 28	169,5	173,21	21	18	0,285 71	0,714 29	151,12	185,82	0,807 89
FVC2000/ Db1/102_8	66	0,829 87	0,121 63	0,730 17	0,249 23	0,487 04	0,239 76	1,087	0,731 32	0,172 33	0,256 14	177,5	180,27	61	45	0,245 9	0,508 2	166,44	197,53	0,783 87
FVC2000/ Db1/102_2	65	0,838 27	0,111 13	0,747 43	0,222 09	0,531 92	0,278 35	1,159	0,647 29	0,144 48	0,215 63	173,43	176,79	67	49	0,223 88	0,597 01	160,78	217,07	0,778 02
FVC2000/ Db1/104_2	65	0,807 99	0,101 09	0,754 92	0,201 47	0,475 31	0,234 79	1,198 2	0,983 29	0,167 3	0,257 11	214,18	216,15	34	28	0,470 59	0,441 18	205,26	178,71	0,735 42
FVC2000/ Db1/106_1	64	0,801 23	0,159 03	0,743 36	0,238 92	0,528 58	0,279 14	1,231 1	0,994 34	0,173 19	0,251 76	203,83	206,18	36	32	0,111 11	0,472 22	193,09	194,64	0,760 31
FVC2000/ Db1/106_8	64	0,720 57	0,241 82	0,670 16	0,299 3	0,509 58	0,297 51	1,163 2	0,733 62	0,212 31	0,272 9	222,33	224,54	35	33	0,114 29	0,371 43	211,82	177,19	0,750 81
FVC2000/ Db1/101_3	63	0,820 69	0,131 03	0,800 81	0,193 21	0,519 36	0,256 45	1,180 5	0,618 31	0,177 84	0,274 07	186,79	190,02	8	8	0,125	1,0	164,42	173,4	0,791 8
FVC2000/ Db1/102_4	63	0,807 02	0,167 41	0,749 13	0,254 48	0,475 63	0,225 25	1,196 6	0,973 38	0,279 06	0,373 27	172,68	175,89	54	49	0,296 3	0,555 56	160,39	221,01	0,767 39
FVC2000/ Db1/102_7	62	0,828 55	0,142 59	0,753 21	0,222 37	0,506 19	0,269 56	1,122 4	0,724 99	0,141 18	0,184 46	181,8	184,09	45	37	0,444 44	0,622 22	168,83	194,65	0,801 04
FVC2000/ Db1/104_5	62	0,780 73	0,149 42	0,749 25	0,218 2	0,528 14	0,283 8	1,091 7	0,754 29	0,169 04	0,248 81	200,11	202,17	36	27	0,444 44	0,583 33	190,32	172,72	0,738 1
FVC2000/ Db1/105_6	61	0,830 39	0,126 23	0,785 37	0,187 72	0,532 62	0,275 87	1,120 6	0,538 63	0,126 07	0,213 24	201,76	205,25	23	20	0,173 91	0,652 17	187,45	209,03	0,777 05

Table A.1 (continued)

Image identifier	$Q_{29794-4}$	$(Q_{OCL}^{\mu})$	$Q_{OCL}^{\sigma}$	$(Q_{LCS}^{\mu})$	$Q_{LCS}^{\sigma}$	$(Q_{FDA}^{\mu})$	$Q_{FDA}^{\sigma}$	$(Q_{RVU}^{\mu})$	$Q_{RVU}^{\sigma}$	$(Q_{OFL}^{\mu})$	$Q_{OFL}^{\sigma}$	$Q_{MU}$	$Q_{MMB}$	$Q_{MIN}^{cnt}$	$Q_{MIN}^{com}$	$Q_{MIN}^{\mu}$	$Q_{MIN}^{ocl}$	$(Q_{AREA}^{\mu})$	$Q_{COH}^{sum}$	$Q_{COH}^{rel}$
FVC2000/ Db1/106_7	61	0,757 8	0,223 12	0,780 9	0,141 87	0,459 26	0,245 33	1,192 2	1,328 7	0,162 76	0,257 92	227,08	228,74	22	22	0,272 73	0,590 91	218,33	186,47	0,754 94
FVC2000/ Db1/105_2	60	0,816 07	0,103 67	0,795 73	0,138 57	0,535 95	0,281 54	1,198 4	0,873 68	0,111 29	0,176 31	161,17	166,32	31	24	0,225 81	0,548 39	145,91	206,03	0,717 88
FVC2000/ Db1/105_5	60	0,796 99	0,194 65	0,785 18	0,199 92	0,524 61	0,267 44	1,127 7	0,693 77	0,146 01	0,238 63	211,21	213,0	14	13	0,142 86	0,857 14	195,98	204,76	0,784 53
FVC2000/ Db1/102_6	59	0,811 31	0,134 93	0,700 07	0,270 64	0,534 36	0,272 7	1,111 8	0,651 71	0,140 04	0,226 48	187,22	189,39	51	41	0,352 94	0,588 24	178,26	206,79	0,763 07
FVC2000/ Db1/106_2	59	0,682 69	0,232 19	0,645 44	0,302 93	0,552 62	0,309 22	1,336 6	1,322 5	0,156 65	0,200 44	203,84	206,54	30	28	0,133 33	0,466 67	186,83	144,82	0,692 92
FVC2000/ Db1/107_3	58	0,684 03	0,181 43	0,701 12	0,226 86	0,573 8	0,311 76	1,216 3	1,013 5	0,191 41	0,230 85	211,42	212,86	12	12	0,0	0,416 67	202,06	139,24	0,630 03
FVC2000/ Db1/15_1	58	0,815 47	0,137 21	0,816 84	0,108 81	0,476 68	0,247 74	1,079 2	0,578 56	0,127 1	0,204 76	191,63	194,59	22	18	0,318 18	0,636 36	180,91	194,62	0,775 37
FVC2000/ Db1/102_3	57	0,842 43	0,112 81	0,685 11	0,292 38	0,588 04	0,322 27	1,242 7	0,872 83	0,153 52	0,210 81	191,29	194,2	37	34	0,162 16	0,513 51	173,58	190,12	0,785 62
FVC2000/ Db1/103_1	57	0,769 88	0,147 35	0,739 88	0,237 4	0,552 89	0,288 78	1,082 4	0,749 05	0,189 54	0,249 84	197,41	200,06	28	26	0,392 86	0,5	186,74	168,66	0,691 22
FVC2000/ Db1/10_8	56	0,848 72	0,120 48	0,756 22	0,236 74	0,490 42	0,260 13	1,228 3	1,069 1	0,145 86	0,233 53	179,34	181,58	21	19	0,190 48	0,761 9	163,18	183,44	0,818 92
FVC2000/ Db1/103_3	56	0,804 96	0,134 33	0,789 59	0,165 74	0,511 68	0,255 87	1,096 2	0,768 69	0,171 18	0,228 81	191,11	194,16	38	31	0,236 84	0,447 37	181,57	201,28	0,726 63
FVC2000/ Db1/102_1	55	0,791 52	0,177 47	0,704 95	0,273 61	0,500 83	0,275 81	1,239 7	1,063 6	0,123 4	0,166 28	177,37	179,52	47	36	0,276 6	0,531 91	161,2	207,98	0,781 88
FVC2000/ Db1/107_7	55	0,755 6	0,155 5	0,748 74	0,201 63	0,474 27	0,258 63	1,111 8	0,708 92	0,149 47	0,219 97	230,61	231,14	14	14	0,285 71	0,857 14	221,27	143,99	0,719 95
FVC2000/ Db1/106_5	54	0,639 11	0,296 04	0,608 32	0,320 55	0,525 76	0,304 26	1,206 7	0,922 38	0,199 74	0,253 97	226,14	228,05	12	12	0,25	0,833 33	213,47	152,17	0,701 23
FVC2000/ Db1/107_5	54	0,752 55	0,146 02	0,707 39	0,240 47	0,475 96	0,266 13	1,054 4	0,635 44	0,127 7	0,194 03	229,86	230,38	20	20	0,4	0,65	224,2	139,71	0,709 21
FVC2000/ Db1/109_3	53	0,736 89	0,181 4	0,618 93	0,318 4	0,524 64	0,288 08	1,183 8	0,879 12	0,164 42	0,269 3	173,16	177,01	39	37	0,461 54	0,538 46	155,52	163,48	0,664 56
FVC2000/ Db1/109_5	53	0,782 22	0,133 36	0,684 9	0,263 65	0,560 52	0,323 51	1,253 6	0,837 95	0,132 76	0,206 37	175,12	179,52	54	46	0,166 67	0,462 96	151,38	164,75	0,710 14
FVC2000/ Db1/100_7	52	0,609 63	0,195 99	0,684 52	0,235 62	0,425 24	0,254 56	1,224 9	0,927 33	0,236 27	0,253 23	208,54	209,65	3	3	0,666 67	0,666 67	208,43	164,49	0,455 66
FVC2000/ Db1/103_6	52	0,752 68	0,180 5	0,773 37	0,170 53	0,564 99	0,267 4	1,104 7	0,680 18	0,190 63	0,241 91	199,97	202,71	23	17	0,391 3	0,521 74	188,97	192,91	0,696 41

Table A.1 (continued)

Image identifier	$Q_{29794-4}$	$(Q_{OCL}^{\mu})$	$(Q_{OCL}^{\sigma})$	$(Q_{LCS}^{\mu})$	$Q_{LCS}^{\sigma}$	$(Q_{FDA}^{\mu})$	$Q_{FDA}^{\sigma}$	$(Q_{RVU}^{\mu})$	$Q_{RVU}^{\sigma}$	$(Q_{OFL}^{\mu})$	$Q_{OFL}^{\sigma}$	$Q_{MU}$	$Q_{MMB}$	$Q_{MIN}^{cnt}$	$Q_{MIN}^{com}$	$Q_{MIN}^{mu}$	$Q_{MIN}^{ocl}$	$(Q_{AREA}^{\mu})$	$Q_{COH}^{sum}$	$Q_{COH}^{rel}$
FVC2000/ Db1/101_4	51	0,770 83	0,167 78	0,764 17	0,226 07	0,585 45	0,270 04	1,182 9	1,226 4	0,257 26	0,356 7	198,3	200,68	10	9	0,1	0,9	177,41	168,31	0,754 76
FVC2000/ Db1/108_4	51	0,756 69	0,173 73	0,669 37	0,297 69	0,660 5	0,320 35	1,267 8	1,179 3	0,158 33	0,233 3	196,12	198,0	32	32	0,062 5	0,25	180,4	153,6	0,704 58
FVC2000/ Db1/105_7	50	0,827	0,140 71	0,782 03	0,189 18	0,544 53	0,279 83	1,106 9	0,584 27	0,122 68	0,192 61	195,53	199,19	25	19	0,08	0,68	181,26	213,17	0,783 73
FVC2000/ Db1/107_2	50	0,762 27	0,145 48	0,780 58	0,139 86	0,560 71	0,289 99	1,257 7	0,877 99	0,146 85	0,234 89	203,74	205,82	18	17	0,222 22	0,666 67	191,96	154,41	0,731 78
FVC2000/ Db1/12_2	49	0,658 65	0,223 61	0,747 69	0,207 97	0,513 65	0,249 34	1,090 6	0,808 5	0,447 61	0,425 57	204,05	206,17	12	12	0,083 333	0,416 67	186,18	115,31	0,686 38
FVC2000/ Db1/30_6	49	0,866 92	0,094 323	0,726 3	0,261 03	0,476 79	0,241 15	1,130 3	0,820 44	0,128 46	0,211 1	182,91	185,17	24	14	0,208 33	0,791 67	171,0	176,22	0,843 16
FVC2000/ Db1/108_7	48	0,716 42	0,195 37	0,607 67	0,316 05	0,579 55	0,323 33	1,330 7	1,114 2	0,163 92	0,236 41	182,45	186,67	34	33	0,176 47	0,441 18	175,75	186,47	0,593 85
FVC2000/ Db1/109_7	48	0,781 17	0,128 05	0,644 32	0,304 52	0,530 32	0,323 99	1,282 1	1,013 5	0,130 97	0,203 79	168,13	173,13	66	58	0,181 82	0,424 24	140,64	153,17	0,680 73
FVC2000/ Db1/108_3	47	0,684 27	0,188 73	0,683 56	0,255 95	0,601 85	0,326 87	1,223 5	1,016 7	0,217 49	0,276 98	192,87	195,64	29	27	0,068 966	0,310 34	169,47	108,4	0,660 97
FVC2000/ Db1/14_3	47	0,709 08	0,201 52	0,715 89	0,268 67	0,578 6	0,285 69	1,177 3	0,938 39	0,227 71	0,310 54	196,09	198,04	10	10	0,0	0,6	175,02	150,36	0,656 61
FVC2000/ Db1/16_7	46	0,633 61	0,243 85	0,675 59	0,264 1	0,613 28	0,303 81	1,206 3	1,036 5	0,207 67	0,227 71	218,74	219,82	7	7	0,571 43	0,857 14	209,81	123,98	0,629 32
FVC2000/ Db1/22_1	46	0,734 09	0,188 66	0,766 47	0,160 75	0,574 27	0,286 1	1,269 8	1,553 3	0,188 91	0,265 65	202,53	204,68	9	9	0,444 44	0,444 44	184,77	125,59	0,761 16
FVC2000/ Db1/15_5	45	0,836 03	0,121 06	0,815 3	0,106 47	0,472 22	0,222 55	1,061 9	0,395 55	0,099 617	0,164 9	209,16	212,54	30	22	0,366 67	0,733 33	186,32	153,29	0,815 4
FVC2000/ Db1/21_4	45	0,639 03	0,183 21	0,683 36	0,249 04	0,619 8	0,324 96	1,127 8	0,797 19	0,194 54	0,249 35	212,03	213,77	6	6	0,0	0,666 67	202,24	115,45	0,583 08
FVC2000/ Db1/108_1	44	0,717 66	0,192 09	0,660 49	0,283 81	0,620 95	0,325 09	1,249 7	1,141 1	0,168 09	0,212 86	178,68	182,4	23	21	0,173 91	0,391 3	154,18	135,91	0,676 18
FVC2000/ Db1/11_3	44	0,739 17	0,185 39	0,704 95	0,271 76	0,537 97	0,294 1	1,119 8	0,797 1	0,135 04	0,217 37	201,83	203,65	7	7	0,0	0,857 14	191,11	153,74	0,692 53
FVC2000/ Db1/110_5	43	0,573 75	0,181 63	0,699 39	0,207 35	0,506 97	0,289 98	1,214 1	0,920 59	0,207 6	0,224 25	208,66	209,55	0	0	—	—	194,98	76,081	0,500 53
FVC2000/ Db1/12_4	43	0,641 25	0,229 43	0,738 32	0,224 14	0,529 66	0,271 3	1,221 1	1,161 6	0,502 19	0,468 54	211,22	212,9	9	9	0,222 22	0,333 33	194,94	98,897	0,691 59
FVC2000/ Db1/13_1	42	0,641 51	0,251 9	0,632 58	0,321 03	0,612 06	0,316 38	1,237 1	1,131 1	0,224 26	0,245 44	213,61	215,5	6	6	0,166 67	0,5	201,42	128,86	0,660 8